Deep-Sea Research I 56 (2009) 1419–1439

Contents lists available at ScienceDirect

Deep-Sea Research I

journal homepage: www.elsevier.com/locate/dsri

The dual isotopes of deep nitrate as a constraint on the cycle and budget of oceanic fixed nitrogen

Daniel M. Sigman [a,*], Peter J. DiFiore [a], Mathis P. Hain [b], Curtis Deutsch [c], Yi Wang [a], David M. Karl [d], Angela N. Knapp [e], Moritz F. Lehmann [f], Silvio Pantoja [g]

[a] Department of Geosciences, Princeton University, Princeton, NJ 08544, USA
[b] Institute of Geosciences, University of Potsdam, PO Box 60 15 53, Potsdam D-14415, Germany
[c] Department of Atmospheric and Oceanic Sciences, University of California, Los Angeles, CA 90095, USA
[d] Department of Oceanography, 1000 Pope Rd. MSB 629, University of Hawaii, Honolulu, HI 96822, USA
[e] Department of Marine and Environmental Biological Sciences, University of Southern California, University of Southern California, 3616 Trousdale Parkway, AHF 108, Los Angeles, CA 90089-0371, USA
[f] Institute for Environmental Geosciences, Bernoullistrasse 30, Universität Basel, CH-4056 Basel, Switzerland
[g] Department of Oceanography and Center for Oceanographic Research in the Eastern South Pacific, University of Concepción, Casilla 160-C, Concepción, Chile

ARTICLE INFO

Article history:
Received 21 January 2008
Received in revised form
4 April 2009
Accepted 21 April 2009
Available online 3 May 2009

Keywords:
Nitrate
Stable isotope
Biogeochemistry
Numerical model
Nutrients

ABSTRACT

We compare the output of an 18-box geochemical model of the ocean with measurements to investigate the controls on both the mean values and variation of nitrate $\delta^{15}N$ and $\delta^{18}O$ in the ocean interior. The $\delta^{18}O$ of nitrate is our focus because it has been explored less in previous work. Denitrification raises the $\delta^{15}N$ and $\delta^{18}O$ of mean ocean nitrate by equal amounts above their input values for N_2 fixation (for $\delta^{15}N$) and nitrification (for $\delta^{18}O$), generating parallel gradients in the $\delta^{15}N$ and $\delta^{18}O$ of deep ocean nitrate. Partial nitrate assimilation in the photic zone also causes equivalent increases in the $\delta^{15}N$ and $\delta^{18}O$ of the residual nitrate that can be transported into the interior. However, the regeneration and nitrification of sinking N can be said to decouple the N and O isotopes of deep ocean nitrate, especially when the sinking N is produced in a low latitude region, where nitrate consumption is effectively complete. The $\delta^{15}N$ of the regenerated nitrate is equivalent to that originally consumed, whereas the regeneration replaces nitrate previously elevated in $\delta^{18}O$ due to denitrification or nitrate assimilation with nitrate having the $\delta^{18}O$ of nitrification. This lowers the $\delta^{18}O$ of mean ocean nitrate and weakens nitrate $\delta^{18}O$ gradients in the interior relative to those in $\delta^{15}N$. This decoupling is characterized and quantified in the box model, and agreement with data shows its clear importance in the real ocean. At the same time, the model appears to generate overly strong gradients in both $\delta^{18}O$ and $\delta^{15}N$ within the ocean interior and a mean ocean nitrate $\delta^{18}O$ that is higher than measured. This may be due to, in the model, too strong an impact of partial nitrate assimilation in the Southern Ocean on the $\delta^{15}N$ and $\delta^{18}O$ of preformed nitrate and/or too little cycling of intermediate-depth nitrate through the low latitude photic zone.

1. Introduction

The mean $\delta^{15}N$ of oceanic fixed N is set by the $\delta^{15}N$ of the input and the net isotopic fractionation of fixed N removal from the ocean. Oceanic N_2 fixation, apparently the dominant source of fixed N to the ocean

* Corresponding author. Tel.: +1 609 258 2194; fax: +1 609 258 5242.
E-mail address: sigman@princeton.edu (D.M. Sigman).

0967-0637/$ - see front matter © 2009 Elsevier Ltd. All rights reserved.
doi:10.1016/j.dsr.2009.04.007

(Gruber, 2004), introduces new fixed N with a $\delta^{15}N$ of ~ -2-0‰ relative to atmospheric N_2 (Carpenter et al., 1997; Delwiche et al., 1979; Hoering and Ford, 1960) ($\delta^{15}N_{sample}$ (in permil, ‰) = $1000((^{15}N/^{14}N)_{sample}/(^{15}N/^{14}N)_{reference}-1)$, where the $^{15}N/^{14}N$ reference is N_2 in air). The removal processes are most importantly water column and sedimentary denitrification (Brandes and Devol, 2002). Studies of the ocean water column have typically yielded estimates of 20-30‰ for the isotope effect for denitrification (Altabet et al., 1999; Brandes et al., 1998; Cline and Kaplan, 1975; Liu and Kaplan, 1989; Sigman et al., 2003b; Voss et al., 2001)(the N isotope effect, $^{15}\varepsilon$, is defined here in units of permil as $1000(^{14}k/^{15}k-1)$, where ^{14}k and ^{15}k are the rate coefficients of the reactions for the ^{14}N- and ^{15}N-bearing forms of NO_3^-, respectively). By contrast, sedimentary denitrification in a variety of environments causes minimal net isotope enrichment of oceanic NO_3^- (Brandes and Devol, 1997, 2002; Lehmann et al., 2004; Lehmann et al., 2007; Sebilo et al., 2003; Sigman et al., 2001).

The isotopic distinction between water column and sedimentary denitrification has been used to develop a constraint on the relative importance of water column versus sedimentary denitrification in the loss of N from the global ocean (Brandes and Devol, 2002; Deutsch et al., 2004) (Fig. 1a). Most of the deep ocean (>2 km) has a NO_3^- $\delta^{15}N$ of 5.0 ± 0.5‰ relative to atmospheric N_2 (Sigman et al., 2000). Given this mean ocean nitrate $\delta^{15}N$ (blue line in Fig. 1a) and assuming a homogenous (i.e. 'one-box') ocean in steady state, an isotope effect of 25‰ for water column denitrification (the vertical offset between the red arrow and blue line in Fig. 1a) would require that water column denitrification accounts for only 20% of the modern loss of fixed nitrogen from the ocean (red arrow in Fig. 1a), with sedimentary denitrification accounting for the remaining 80% (grey arrow in Fig. 1a). There are important additional considerations regarding the isotopic impacts of both water column and sedimentary denitrification (e.g., Deutsch et al., 2004; Lehmann et al., 2007), and the implied total denitrification rate appears far greater than the estimated N_2 fixation rate, an unlikely scenario of extreme imbalance (Brandes and Devol, 2002). Nevertheless, even as our understanding of specific N fluxes and their distributions change, the steady state budget approach is likely to remain useful.

Reporting the first published measurements of nitrate O isotopes in the ocean, Casciotti et al. (2002) observed that nitrate $\delta^{18}O$ in the subarctic North Pacific varies little with depth in the ocean interior. It also appeared from those data that the $\delta^{18}O$ of deep nitrate is similar to that of ambient water, although this was recognized to be uncertain because of poor isotopic definitions for the available reference materials. With subsequent revisions in the assigned oxygen isotope ratios of international reference materials (Böhlke et al., 2003), it now appears that the nitrate $\delta^{18}O$ in the deep North Pacific is 1.5-2.0‰ greater than the $\delta^{18}O$ of ambient deep water (Casciotti et al., 2008). Regardless, deep nitrate $\delta^{18}O$ is much closer to the $\delta^{18}O$ of ambient water than to that of ambient O_2, which is >20‰ higher than the nitrate in the same water.

The O isotopic homogeneity of the nitrate profile from the subarctic North Pacific immediately suggested that water, not O_2, was the dominant source of O atoms in nitrate, as the $\delta^{18}O$ of O_2 varies significantly in the ocean interior because of fractionation during respiration (Bender, 1990). The similarity of the absolute isotopic ratio to water was also suggestive of a water source. However, this was known to be a weak constraint, for three reasons. First, there may be large fractionations in the incorporation of O atoms into nitrate, so isotopic similarity is not a compelling indicator of source. Second, deep ocean nitrate is not derived solely by regeneration of organic N and oxidation (nitrification) to nitrate. Roughly half of deep nitrate in the North Pacific is "preformed," originating from the water parcel's surface source region, where fractionation during nitrate assimilation may have occurred. Third, denitrification may also influence the nitrate in the deep ocean, especially within the Pacific.

It is informative to generate a whole-ocean steady state nitrate budget as experienced by its oxygen atoms, analogous to the budget described above for N in nitrate (Fig. 1b). In this case, the input is oxidation of reduced N to nitrate, that is, nitrification, composed of ammonium oxidation to nitrite and nitrite oxidation to nitrate. This includes the nitrification of newly fixed N. As described above, the $\delta^{18}O$ of newly produced nitrate from nitrification is not well known but appears to be close to the $\delta^{18}O$ of the ambient water (<2‰ greater than the $\delta^{18}O$ of ambient water, based on current measurements for international reference materials (Böhlke et al., 2003)) ($\delta^{18}O_{sample} = 1000((^{18}O/^{16}O)_{sample}/(^{18}O/^{16}O)_{reference}-1)$, where the reference is Vienna Standard Mean Ocean Water (VSMOW)). From the perspective of the oxygen isotopes of nitrate, both denitrification and nitrate assimilation are absolute sinks. Thus, in contrast to the case for the N isotopes, the O isotope steady state diagram requires three loss terms: water column denitrification, sedimentary denitrification, and nitrate assimilation (Fig. 1b). Culture studies of algal nitrate assimilation and denitrification indicate strong coupling between these two isotope systems, with NO_3^- $\delta^{15}N$ and $\delta^{18}O$ increasing nearly equally as consumption proceeds (Granger et al., 2008; Granger et al., 2004). If we assume O isotope effects of 25‰ and 0‰ for water column and sedimentary denitrification and 5‰ for nitrate assimilation (e.g., Brandes et al., 1998; Sigman et al., 1999) and take the water column-to-sedimentary denitrification ratio from the N isotopes as described above (1:4), then the one-box model of the ocean predicts a mean ocean nitrate $\delta^{18}O$ that is 5‰ greater than that of the nitrification input (Fig. 1b).

However, for the above isotope effects, we expect 5‰ to be too high for the ^{18}O enrichment of mean ocean nitrate above its nitrification value, most importantly because nitrate is commonly consumed to high degrees by algal assimilation in the surface ocean. For fractionation during assimilation to be "expressed" in the $\delta^{18}O$ of nitrate in the ocean interior (i.e., for the fractionation due to this process to impact the $\delta^{18}O$ of nitrate in the interior), there must be only partial nitrate consumption followed by physical transport of the residual (preformed) nitrate into the interior (Fig. 2a). If nitrate is upwelled or

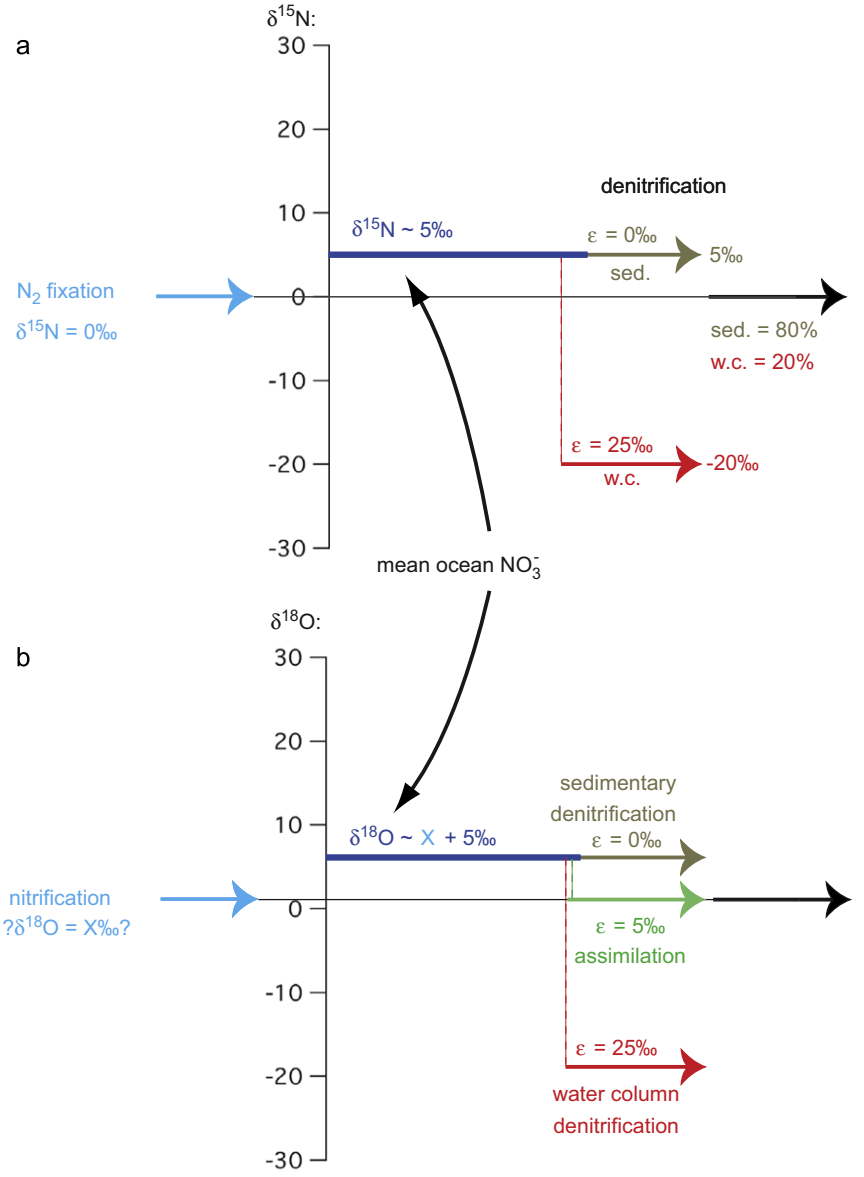

Fig. 1. One-box model views of the budgets of the (a) nitrogen isotopes and (b) oxygen isotopes of nitrate in the ocean. The assumed isotope effects are representative values (see text). For simplicity, a $\delta^{15}N$ of 0‰ for N_2 fixation is used here, even though a value of −1‰ is used in the model. The $\delta^{18}O$ of nitrate from nitrification is left unspecified here (X) but, as discussed in the text, appears to be <2‰ higher than ambient seawater. The N budgets constructed here are known or suspected to be incorrect because they do not account for gradients in nitrate concentration and isotopic composition in the ocean, which represents one the central motivations for this study.

mixed into the surface and then completely consumed, there will be no isotopic expression of assimilation at the regional or whole-ocean scale (Fig. 2b). In the case of complete nitrate consumption, the O isotopic effect of nitrate assimilation and its coupling to nitrification resembles that of sedimentary denitrification and its coupling to N_2 fixation plus nitrification: both sets of processes remove nitrate with minimal nitrate O isotope enrichment and replace it with nitrate with the $\delta^{18}O$ of nitrification. However, the nitrate assimilation/nitrification couple has no direct effect on the $\delta^{15}N$ of mean ocean nitrate. In short, the mean value of and spatial gradients in nitrate $\delta^{18}O$, when coupled to those of nitrate $\delta^{15}N$, should provide a constraint on the relative rates of (1) water column denitrification, (2) sedimentary denitrification, (3) nitrate assimilation occurring to completion, and (4) nitrate assimilation that only partially consumes its gross nitrate supply.

The effort to interpret both the mean isotopic composition and the isotopic gradients of nitrate in the ocean calls for a quantitative model that takes into account not only the relevant biogeochemical fluxes in the ocean N

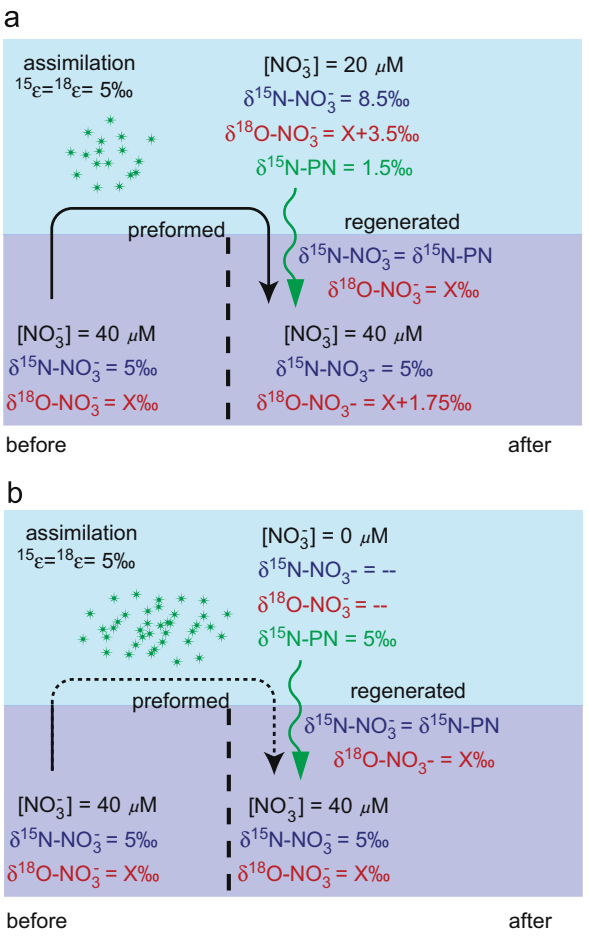

Fig. 2. The change in subsurface nitrate δ^{15}N and δ^{18}O due to nitrate assimilation in the sunlit surface ocean for the cases of (a) 50% consumption and (b) complete consumption of the upwelled nitrate. A subsurface water parcel (shown on the lower left of both a and b) is advected into the photic zone (shown in lighter blue), undergoes nitrate consumption by algae, and is then advected back into the subsurface (on the lower right of both a and b). The organic N produced from the consumed nitrate ("PN" for particulate N) eventually sinks into the subsurface, where it is regenerated back to nitrate. Here as elsewhere in this manuscript, we assume that nitrate assimilation occurs with equal N and O isotope effects ($^{15}\varepsilon$ and $^{18}\varepsilon$) of 5‰ for nitrate assimilation. For the purposes of this calculation, we assume that nitrification in the subsurface produces nitrate with a δ^{18}O of X‰ and with a δ^{15}N equivalent to the organic N being regenerated. We also assume here that deep nitrate starts with a δ^{18}O of X‰, in order to show how deep nitrate is changed from the δ^{18}O of regeneration by partial nitrate assimilation. We note two simplifications: (1) the δ^{18}O of nitrate in the interior starts at the nitrification value, and (2) remineralization occurs entirely in the newly subducted water. (For interpretation of the references to colour in this figure legend, the reader is referred to the web version of this article.)

cycle and budget but also the structure and circulation of the ocean. As a first step in this direction, to a geochemical multi-box model of the ocean (Keir, 1988; Sigman et al., 2003a, 1998), we have added a simple N cycle and budget as well as the N and O isotope systematics that appear to accompany them. The output from the model provides insight into the impacts that different aspects of the N cycle have on the mean values and distributions of nitrate δ^{15}N and δ^{18}O in the ocean, given the information currently available on the isotope systematics of the relevant processes and in the context of the small but growing body of data. Below, we describe the isotopic distributions predicted by the model and compare the model output to water column profiles from different basins of the global ocean, with emphasis on comparing the N and O isotopes of nitrate.

In this study, we focus on the nitrate in the ocean interior, below the thermocline. The motivation for this choice is two-fold. First, the ocean interior is the dominant source of nitrate to the upper ocean (N_2 fixation being the most notable other N input) and thus sets the "starting point" from which the nitrate isotopes in the thermocline and surface mixed layer evolve. Second, in their own right, the mean ocean nitrate isotope values and inter-basin gradients deserve attention as possible constraints on ocean biogeochemistry.

2. Methods

2.1. Model description

Our nitrate isotope model is incorporated into a numerical box model with architecture and circulation from the CYCLOPS box model (Fig. 3) (Keir, 1988; Sigman et al., 2003a, 1998). Below, after describing modifications to the model architecture, we describe the basic controls and isotopic characteristics of the fluxes that constitute the model of the global ocean N cycle, as well as the steady state N budget that results from the model. The dynamics of the ocean N cycle model and the sensitivities that result will be described in more detail elsewhere.

2.1.1. Model architecture

From the original CYCLOPS (Keir, 1988), the Southern Ocean has been modified to better simulate its component regions. The original surface Southern Ocean box has been subdivided into three boxes: (1) the "polar" Antarctic Zone surface (PAZ; roughly speaking, from Antarctica to 65°S), intended to represent the Antarctic south of the Southern Antarctic Circumpolar Front (SACCF); (2) the "open" Antarctic surface (AZ, 65°S to 50°S), intended to represent the Antarctic between the SACCF and the Subantarctic Front; and the Subantarctic Zone surface (SAZ, 50°S to 42°S; added previously (Robinson et al., 2005)). The total Southern Ocean surface area has been increased to account for these changes (Orsi et al., 1995). The circulation and export production/regeneration schemes associated with the modified model are shown in Fig. 3.

2.1.2. Export production and N_2 fixation

Following previous applications of CYCLOPS, export production is controlled by phosphate supply, based here on model-prescribed phosphate concentrations for the surface boxes. In the low latitude surface boxes, the gross phosphate supply is essentially completely consumed into

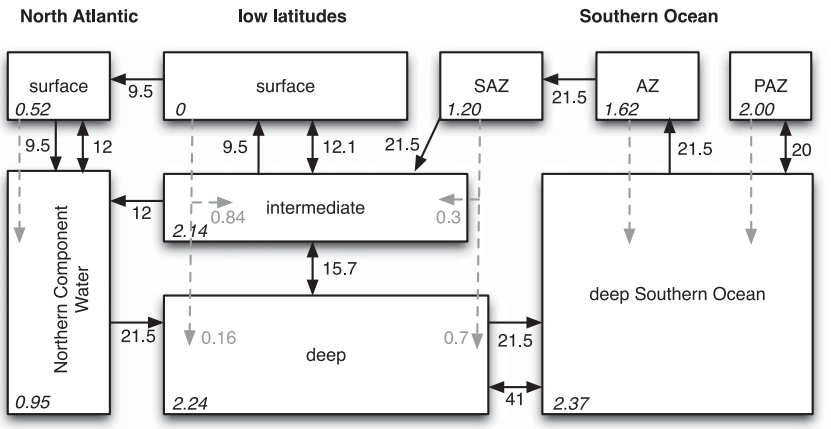

Fig. 3. Diagram of the architecture and circulation of the modified CYCLOPS ocean geochemical box model (Keir, 1988), collapsing the Atlantic, Indian, and Pacific basins into one set of surface, intermediate, and deep boxes in order to focus on the modifications to the Southern Ocean surface. Circulation is shown in black arrows. The Southern Ocean components of the CYCLOPS model have been attributed to the different Southern Ocean surface boxes as follows: the 20 Sv of vertical mixing and deep water formation occurs in the PAZ, the 21.5 Sv of Ekman driven upwelling occurs in the AZ, and convergence-associated subduction into the intermediate boxes occurs in the SAZ. The fates of export production from the surface boxes are shown in dashed gray arrows. These follow the original CYCLOPS model, except for the export from the SAZ, which enters the low latitude intermediate and deep boxes, with strong preferential (70%) transport to the deep boxes because the intermediate boxes are interpreted to shoal under the SAZ. The italicized value in the lower left of each box indicates its $[PO_4^{3-}]$ in μmol/kg.

organic matter and exported into the ocean interior. The fixed N cycle is simplified in the model, including only nitrate and particulate N. Nitrate is assimilated into organic matter in a 16:1 ratio to phosphate. Nitrate assimilation is assumed to proceed with an isotope effect of 5‰ for both the N and O isotopes (Granger et al., 2004; Sigman et al., 1999).

If the gross nitrate supply to a surface box is insufficient to allow for export production with a N:P ratio of 16:1, then N_2 fixation occurs to satisfy that criterion (Deutsch et al., 2007; Tyrrell, 1999). In the model, 'fixation' adds nitrate with a $\delta^{15}N$ of −1‰, which is then followed by complete assimilation of both the original nitrate supply and the newly 'fixed' nitrate. In the case of complete nitrate consumption (always the case when N_2 fixation is activated), there is essentially no expression of the isotope effect of nitrate assimilation.

2.1.3. Regeneration and nitrification

Regeneration completely returns exported organic material to the water column as dissolved components. The routing of sinking organic matter into the ocean interior boxes and its regeneration are taken from Keir (1988), with minor modifications related to the Southern Ocean (Fig. 3). Organic matter regeneration/nitrification is assumed to yield nitrate with the $\delta^{15}N$ of the sinking organic matter. In the model experiments below, two alternatives are considered for the $\delta^{18}O$ of newly regenerated nitrate. In the standard case, the nitrate O atoms derive solely from ambient water, so that its $\delta^{18}O$ is directly related to the water in which nitrification is occurring. For simplicity in presenting the results, we assume that nitrification produces nitrate with a $\delta^{18}O$ equivalent to the ambient water, but we account for an apparent offset when comparing with data. The $\delta^{18}O$ of seawater is prescribed for each of the surface boxes based on a simple relationship to salinity ($\Delta\delta^{18}O/\Delta S = 0.5‰$/psu; with a $\delta^{18}O$ of 0‰ at S of 34.7 psu) and is conserved in the ocean interior, comparing passably with a global database (LeGrande and Schmidt, 2006). In the alternative case, it is assumed that five sixths of the O atoms in nitrate derive from water while the remaining one sixth derives from dissolved O_2 (see discussion in Casciotti et al., 2002). We assume that the nitrate O atoms deriving from ambient O_2 have the same $\delta^{18}O$ as the O_2. The $\delta^{18}O$ of the O_2 is prescribed in the surface ocean at a uniform value of 24.2‰ vs. VSMOW, and the isotope effect associated with aerobic respiration in the interior is assumed to be 18‰ (Bender, 1990; but see Levine et al., 2009).

2.1.4. Water column denitrification

To simulate reasonable sensitivities for denitrification within suboxic zones and to include the isotope dynamics associated with partial consumption of nitrate in the regions of water column denitrification (Deutsch et al., 2004), we have developed a relatively detailed parameterization of the suboxic regions (Appendix A). Since nitrite and other redox intermediates are not included in this model, denitrification is equivalent here to respiratory (i.e. dissimilatory) reduction of nitrate, with one exception: it is assumed that the N within the organic matter fueling the denitrification is completely consumed in the denitrification process (e.g., by anammox (Kuypers et al., 2005)).

Denitrification within the suboxic zone is assumed to have an organism-scale isotope effect of 25‰ for both the nitrogen and oxygen atoms of the nitrate consumed (Brandes et al., 1998; Granger et al., 2008). The "dilution effect", the under-expression of the organism-scale isotope effect resulting from mixing water of different nitrate concentrations and isotopic compositions (Deutsch et al.,

2004), occurs at two steps: by exchange first between a suboxic core region and its surrounding oxygen minimum volume and second between the oxygen minimum and the regular ocean box (Appendix A).

2.1.5. Benthic denitrification

Our parameterization of the rate of benthic denitrification follows a simple dependency on the rate of organic matter flux to the sediment (Middelburg et al., 1996) (Appendix A). In benthic denitrification, we assume an effective isotope effect of zero for the consumption of both nitrate N and O isotopes, which is appropriate but a simplification of actual findings (Brandes and Devol, 1997, 2002; Lehmann et al., 2004, 2005, 2007).

2.2. Denitrification rates in the model's standard case

The model's rates of water column and sedimentary denitrification are 36.8 and 99.1 Tg N yr^{-1}, respectively, the sum of which is balanced by N_2 fixation (Table 1). While the ratio of rates is roughly similar to estimates (Brandes and Devol, 2002; Deutsch et al., 2004), the total denitrification rate is significantly less than recent estimates (Deutsch et al., 2001), roughly by a factor of 2 (Gruber and Sarmiento, 1997). This is primarily due to the export production of the model (512 Tg N yr^{-1}), which is roughly half that of some recent estimates based on satellite data (Laws et al., 2000) (see Appendix A regarding the organic carbon flux for sedimentary denitrification); the tendency of box models to have low export production has been discussed previously (Matsumoto et al., 2002).

The model's water column denitrification occurs almost entirely in the intermediate North Pacific box (at 32.4 Tg N yr^{-1}), failing to simulate significant denitrification in the South Pacific and Arabian Sea. CYCLOPS errs toward having overly high [O_2] in the intermediate Indian and South Pacific (Fig. 4 of Keir, 1988). Nevertheless, the real North Pacific does dominate the global volume of water with [O_2] of less than 10 μM (Conkright et al., 2002). The failure of the model to produce significant denitrification rates in the South Pacific and Arabian Sea speaks to the importance of local oceanographic processes in generating specific zones of suboxia and denitrification.

2.3. Nitrate O and N isotope data

We compare our model results with a handful of depth profiles of nitrate O and N isotopes from the global ocean (Table 2, Fig. A1): (1) the subtropical North Atlantic (Atl) (Knapp et al., 2008), (2) the western Mediterranean Sea (Med) (Pantoja et al., 2002), (3) the Antarctic Zone of the Southern Ocean in the Indo-Pacific sector (SO), (4) the subtropical North Pacific (HOT station Aloha; (Sigman et al., 2009)), (5) the Bering Sea (BS) (Lehmann et al., 2005), and (6) the eastern tropical North Pacific, off the coast of Baja California (ETNP) (Sigman et al., 2005). The $^{15}N/^{14}N$ and $^{18}O/^{16}O$ of NO_3^- were determined using the denitrifier method (Casciotti et al., 2002; Sigman et al., 2001). In Appendix B, details are given regarding the isotope methods, the ancillary data (nutrient concentrations, preformed nutrient calculations, etc.), and the generation of average isotope values from profile samples (Table 2).

3. Model experiments and results

The N fluxes in the ocean are usefully distinguished as involving the internal cycling of nitrate (nitrate assimilation, N export from the surface ocean, and nitrification in the interior) or the ocean's input/output budget of fixed N (N_2 fixation (followed by nitrification) and denitrification). Since one can think of the internal cycle as the origin of the differences between nitrate N and O isotope behavior, we first describe its effects alone, in a set of experiments in which N_2 fixation and denitrification are inactive (set I, "N cycle only" in Table 3). We then consider some of the same experiments, but in which N_2 fixation and denitrification are active (set II, "with N budget" in Table 3). Within both sets, "Standard" simulations use the baseline circulations, biogeochemistry, and N and O isotope rules.

One goal of our study is to understand the impact of partial nitrate assimilation in polar regions on the N and O isotopes of nitrate in the ocean interior. As an aid in diagnosing this impact, we perform "no assimilation fractionation" experiments (I.B. and II.B., Table 3), in which the N and O isotope effects of nitrate assimilation are set to zero. In addition, for purposes of illustration, a "uniform Southern Ocean" experiment is run in set I (I.C., Table 3) in which a uniform phosphate concentration (that of the open Antarctic from the standard case; $[PO_4^{3-}] = 1.62$ μmol/kg) is applied to all three of the Southern Ocean surface boxes (open Antarctic, polar Antarctic, and Subantarctic).

To provide insight into the possibility that O_2 is incorporated into nitrate during nitrification, "O_2 influence" experiments (I.D. and II.C.) assume that one-sixth of O atoms in nitrate derive from O_2 (I.D. and II.C; I.E. and II.D combine the "no assimilation fractionation" and "O_2 influence" experiments). The "O_2 influence" experiment for the "with N budget" case (II.C) is discussed in Section 3.2.3, while this experiment for the "N cycle only" case (I.D.) is relegated to Appendix C.

3.1. The model with internal N cycling only

3.1.1. Inter-box nitrate $\delta^{18}O$ variations

The $\delta^{18}O$ of nitrate shows a negative correlation with [PO_4^{3-}] (and thus [NO_3^-]) (Fig. 4b, filled symbols; we use [PO_4^{3-}] in our plotting and description of inter-box variations, as [NO_3^-] includes effects of N_2 fixation and denitrification, which are included in the model experiments of Section 3.2.). A negative correlation is also observed between nitrate $\delta^{18}O$ and the ratio of regenerated to total phosphate (Fig. 4f). In contrast, with the isotope effect of nitrate assimilation set to zero, the $\delta^{18}O$ of nitrate is nearly homogenous in the interior, and the mean value is indistinguishable from the assumed $\delta^{18}O$ of newly produced nitrate (Fig. 4b, f, open symbols; slight variations are due to variable water $\delta^{18}O$, which is on

Table 1
Standard case model output.

Box level	Name	Conditions		Concentrations			Isotopes				Fluxes			
		temp. (°C)	sal. (psu)	NO_3^-	PO_4^{3-} (μmol/kg)	O_2	NO_3^- $\delta^{15}N$ (‰ vs. air)	NO_3^- $\delta^{18}O$	H_2O $\delta^{18}O$ (‰ vs. SMOW)	O_2 $\delta^{18}O$	export	N_2 fixation	w.c. denit. (Tg N/yr)	sed. denit.
Standard case model – internal nitrogen cycle only														
Surface	Atlantic	18.5	36.0	0.016	0.001	232.0	34.88	30.20	0.70	24.20	90.7			
	Indian	18.5	35.0	0.016	0.001	233.6	37.69	33.16	0.17	24.20	72.7			
	S. Pacific	18.5	35.0	0.016	0.001	233.6	40.34	35.86	0.17	24.20	79.8			
	N. Pacific	18.5	34.5	0.016	0.001	234.4	33.57	28.90	−0.10	24.20	99.5			
	Boreal (N. Atl.)	4.0	35.0	8.8	0.55	320.7	6.08	1.56	0.17	24.20	1.1			
	Open Antarctic	0.0	33.8	25.9	1.62	365.4	5.84	2.22	−0.47	24.20	84.0			
	Subantarctic	5.0	34.0	19.5	1.22	314.2	7.12	3.50	−0.37	24.20	62.5			
	Polar Antarctic	0.0	33.5	32.0	2.00	366.3	4.89	1.28	−0.63	24.20	23.0			
Intermediate	Atlantic	8.3	34.5	28.6	1.79	167.3	5.99	1.44	−0.08	31.53				
	Indian	7.5	34.3	34.9	2.18	135.5	5.57	1.18	−0.23	34.78				
	S. Pacific	8.2	34.3	35.2	2.20	120.2	5.41	1.07	−0.22	34.07				
	N. Pacific	10.0	34.3	43.9	2.74	12.5	5.06	0.51	−0.20	48.70				
Deep	Boreal (N. Atl.)	5.6	34.8	16.0	1.00	265.2	6.00	1.47	0.08	25.90				
	Atlantic	5.5	34.7	23.2	1.45	227.1	5.38	1.17	−0.02	28.17				
	Southern	4.0	34.2	34.5	2.16	202.5	4.52	0.91	−0.26	30.16				
	Indian	4.6	34.2	37.7	2.36	163.5	4.61	0.86	−0.26	33.42				
	S. Pacific	5.6	34.2	40.0	2.50	126.5	4.66	0.76	−0.25	34.79				
	N. Pacific	6.3	34.3	41.8	2.61	97.9	4.74	0.69	−0.24	36.89				
										Total:	512.0			
Standard case model – with nitrogen budget														
Surface	Atlantic	18.5	36.0	0.016	0.001	232.0	32.03	30.54	0.70	24.20	90.7	43.3	0.0	28.1
	Indian	18.5	35.0	0.016	0.001	233.6	34.95	33.40	0.17	24.20	72.7	22.9	0.0	12.2
	S. Pacific	18.5	35.0	0.016	0.001	233.6	38.50	36.72	0.17	24.20	79.7	28.2	0.0	13.8
	N. Pacific	18.5	34.5	0.016	0.001	234.4	33.82	31.72	−0.10	24.20	99.4	41.6	0.0	15.5
	Boreal (N. Atl.)	4.0	35.0	7.3	0.55	320.7	4.19	2.27	0.17	24.20	1.0	0.0	0.0	0.0
	Open Antarctic	0.0	33.8	20.5	1.62	365.4	4.68	3.17	−0.47	24.20	83.5	0.0	0.0	0.0
	Subantarctic	5.0	34.0	14.1	1.22	314.2	6.31	4.80	−0.37	24.20	62.5	0.0	0.0	0.0
	Polar Antarctic	0.0	33.5	26.6	2.00	366.3	3.54	2.03	−0.63	24.20	22.5	0.0	0.0	0.0
Intermediate	Atlantic	8.3	34.5	23.8	1.78	168.2	4.08	2.13	−0.08	31.53			0.6	3.2
	Indian	7.5	34.3	29.7	2.18	136.2	3.61	1.67	−0.23	34.73			1.3	1.6
	S. Pacific	8.2	34.3	28.8	2.20	122.6	4.66	2.34	−0.22	34.11			2.2	1.9
	N. Pacific	10.0	34.3	32.3	2.74	22.1	7.56	4.44	−0.20	47.12			32.4	1.8
Deep	Boreal (N. Atl.)	5.6	34.8	13.3	1.00	265.5	4.09	2.17	0.08	25.90			0.0	0.0
	Atlantic	5.5	34.7	19.5	1.45	227.7	3.56	1.80	−0.02	28.17			0.0	2.5
	Southern	4.0	34.2	29.1	2.16	203.8	3.10	1.60	−0.26	30.16			0.0	0.0
	Indian	4.6	34.2	31.6	2.36	164.7	3.05	1.44	−0.26	33.40			0.1	6.4
	S. Pacific	5.6	34.2	32.5	2.50	129.2	3.90	1.90	−0.25	34.85			0.3	11.1
	N. Pacific	6.3	34.3	33.6	2.61	101.7	4.47	2.21	−0.24	37.01			0.0	1.2
										Total:	512.0	135.9	36.8	99.1

Table 2
Nitrate isotope station data.

Station	Location	Cruise	NO_3^- $\delta^{15}N$			NO_3^- $\delta^{18}O$		
			Intermediate[a]	Deep[b]	Deep subset[c]	Intermediate[a]	Deep[b]	Deep subset
subtropical N. Atlantic	19.4°N, 65.0°W	BVAL 32	5.0	5.0	4.9	1.8	1.8	1.9
Pacific Antarctic	56.9°S, 139.9°E	CLIVAR SR3	–	4.7	4.8	–	1.9	1.8
subtropical N. Pacific	22.8°N, 157.9°W	HOT 120	6.4	5.3	5.1	2.9	2.0	1.9
Bering Sea	54.8°N, 179.7°E	WAGB 20	5.6	5.4	5.4	2.1	2.2	2.1
eastern tropical N. Pacific	23.5°N, 111.5°W	OXMZ01MV	8.9	–	–	6.1	–	–
western Mediterranean	36.6°N, 0.3°W	ALMOFRONT II	–	3.0	3.1	–	2.6	3.1

[a] 300–1500 m where appropriate. Depth- and nitrate concentration-weighted. Antarctic and western Mediterranean lack an intermediate water type.
[b] 1500 m-bottom. Depth- and nitrate concentration-weighted. The ETNP data set is from the North American margin, lacking waters below 1500 m.
[c] Four consecutive samples from each station, taken from near the profile base, were averaged. The different stations were analyzed together on individual days to more precisely compare the stations. This comparison was performed four times, and the samples from each station were averaged. 95% confidence intervals for deep subset values are estimated to be ±0.1‰ ($\delta^{15}N$) and ±0.3 ($\delta^{18}O$).

Table 3
Model experiments, mean ocean isotope output, and relevant sections and figures

Experiment	NO_3^- $\delta^{15}N$[a]	NO_3^- $\delta^{18}O$[b]	Section	Base figures	Additional figures
I. N cycle only			3.1		
A. standard	5.00	0.89	3.1	4 a, b, e, f; solid symobls	
B. no assimilation fractionation	5.00	−0.20	3.1	4 a, b, e, f; open symobls	
C. uniform Southern Ocean	5.00	1.04	3.1	5	
D. O_2 influence	5.00	6.86	App. C	4 d, h; solid symobls	
E. (B+D)	5.00	5.76		4 d, h; open symobls	
II. With N budget			3.2		
A. standard	4.27	2.20	3.2.1	6 a, b, e, f, i, j; solid symbols	7 a solid symbols; 8
B. no assimilation fractionation	4.59	1.17	3.2.2	6 a, b, e, f, i, j; open symbols	7 a, open symbols
C. O_2 influence	4.27	8.24	3.2.3	6 d, h, l; solid symbols	7 b, solid symbols
D. (B+C)	4.59	7.20		6 d, h, l; open symbols	7 b, open symbols

[a] In ‰ vs. atmospheric N_2 (set in the case of "N cycle only").
[b] In ‰ vs. VSMOW (to be compared with the mean $\delta^{18}O$ of the model ocean water, −0.23‰, and the $\delta^{18}O$ of dissolved O_2, Table 1).

average -0.23‰ vs. VSMOW in the model). These observations are explained as follows. In the standard case, the nitrate $\delta^{18}O$ of a newly formed subsurface water parcel (that is, the parcel's preformed nitrate $\delta^{18}O$) has been elevated by algal assimilation of nitrate that had occurred in the surface. The $\delta^{18}O$ of nitrate added by the regeneration of sinking organic matter is lower than this preformed nitrate $\delta^{18}O$ and thus lowers the $\delta^{18}O$ of nitrate toward the nitrification value as it increases the concentration of nitrate (and phosphate) in aging subsurface water. To capture the dominant regional patterns in this explanation, partial nitrate assimilation in the open Antarctic Zone and Subantarctic Zone surface produces high-$\delta^{18}O$ nitrate, which is then advected into the intermediate boxes (Fig. 3). This high-$\delta^{18}O$ nitrate is then folded into the deep ocean by North Atlantic Deep Water formation, with subsequent addition of regenerated nitrate working to lower nitrate $\delta^{18}O$ as water circulates into the Indo-Pacific.

However, the negative correlation of nitrate $\delta^{18}O$ with the fraction of regenerated phosphate is not perfect. Among the deep ocean boxes, the Southern Ocean has a relatively low $\delta^{18}O$ considering its relatively low fraction of regenerated phosphate. In addition, the global intermediate boxes have a higher mean $\delta^{18}O$ than do the global deep boxes. In contrast, assuming a less realistic version of the Southern Ocean nutrient field, with only a single nutrient concentration in the Southern Ocean surface (I.B., Table 3), a nearly perfect negative correlation is observed among all of the interior boxes (Fig. 5b). The source of the complexity in the standard version of the model is that the Southern Ocean produces subsurface water from two different preformed nitrate concentrations (Fig. 3), with correspondingly different values for nitrate $\delta^{18}O$. These different preformed conditions lead to different trends for $\delta^{18}O$ versus $[PO_4^{3-}]$ and versus regenerated-to-total $[PO_4^{3-}]$, one trend that originates from SAZ conditions (lower $[PO_4^{3-}]$, higher $\delta^{15}N$ and $\delta^{18}O$) and develops in the intermediate boxes and another trend that originates from PAZ conditions (higher $[PO_4^{3-}]$, lower $\delta^{15}N$ and $\delta^{18}O$) and develops in the deep boxes. In experiment I.B., with only a single Southern Ocean surface nutrient concentration, the $\delta^{18}O$ of preformed nitrate entering into both the deep Southern Ocean and the intermediate boxes has a single relationship with nitrate utilization in the surface, producing a single nitrate $\delta^{18}O$-to-fractional regenerated nitrate relationship in the ocean interior (Fig. 5b).

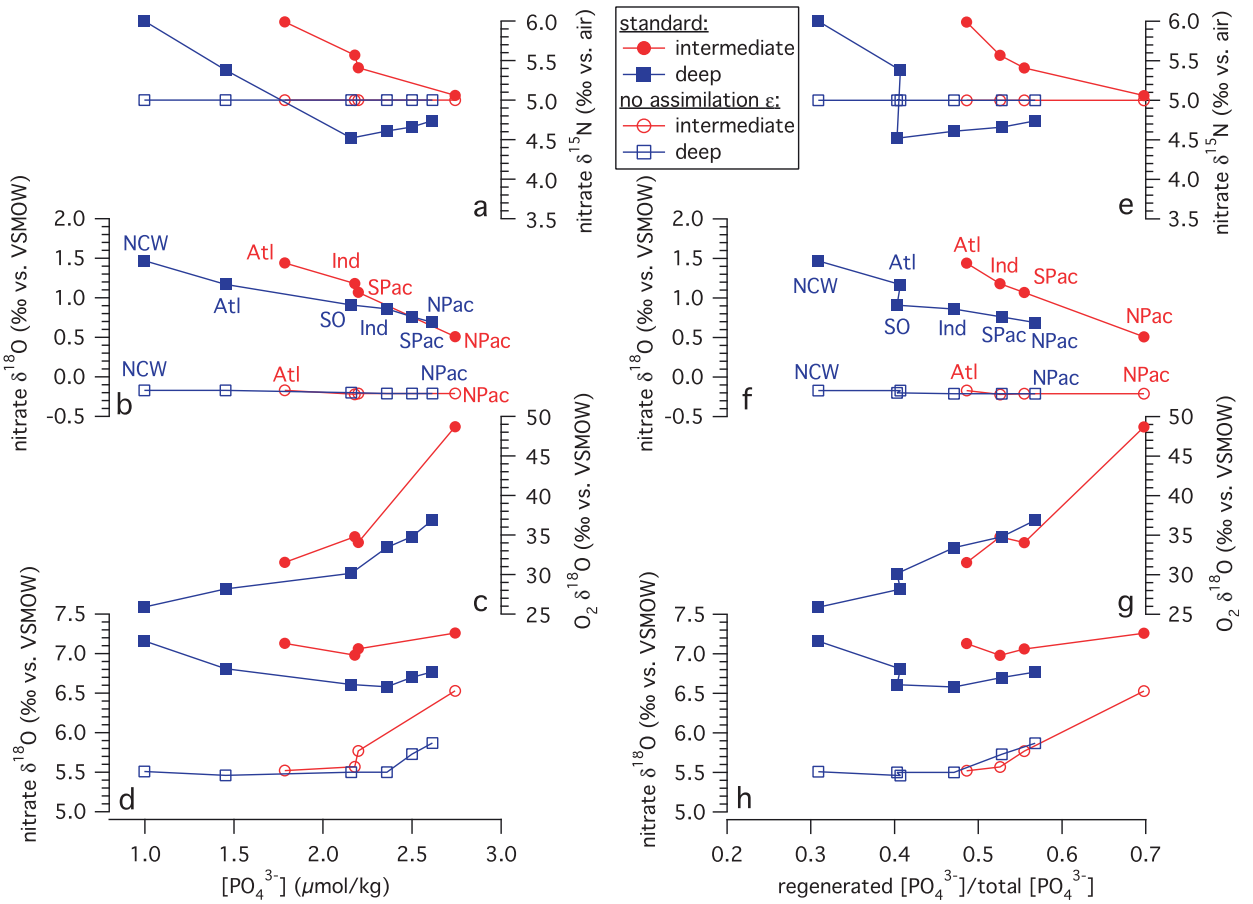

Fig. 4. For the version of the model including only the internal N cycle of the ocean (no N_2 fixation, no denitrification), model output for subsurface box nitrate $\delta^{15}N$ (a, e), nitrate $\delta^{18}O$ (b, f, d, h), and O_2 $\delta^{18}O$ (c, g). Red circles, filled and open, indicate intermediate boxes, while blue squares indicate deep boxes. Model boxes are connected by a line to adjacent boxes (deep: North Atlantic – Atlantic – Southern Ocean – Indian – South Pacific – North Pacific; intermediate: Atlantic – Indian – South Pacific – North Pacific). The isotopic parameters are plotted against both the model's phosphate concentrations (a – d) and its ratio of regenerated to total phosphate concentration ("regenerated" denoting phosphate that entered the subsurface by regeneration from surface-exported organic matter). Output in (b) and (f) are from the model cases where all O atoms in nitrate are inherited from ambient water, while that in (d) and (h) is from the model cases were one out of six oxygen atoms is inherited from ambient dissolved O_2. Filled symbols are from model cases run with the standard nitrate assimilation isotope effects. Open symbols are from model experiments in which $^{15}\varepsilon$ and $^{18}\varepsilon$ of nitrate assimilation are set to 0‰ (rather than 5‰). Relative to Table 3, the filled symbols in (a, b, e, f) are from experiment I.A., while the open symbols in (a, b, e, f) are from I.B. The filled symbols in (d, h) are from experiment I.D., while the open symbols in (d, h) are from I.E. (For interpretation of the references to colour in this figure legend, the reader is referred to the web version of this article.)

This analysis begs the question of why the North Atlantic-sourced water does not imprint its own independent nitrate $\delta^{18}O$ vs. regenerated/total $[PO_4^{3-}]$ relationship on the ocean interior; if it did, the uniform Southern Ocean case would not yield a single trend in $\delta^{18}O$ vs. regenerated/total $[PO_4^{3-}]$ (Fig. 5b). In the model, the nitrate assimilation rate in the North Atlantic surface is only 2.8% of the gross nitrate supply rate, so that it does not produce a significant isotopic signal. Rather than being generated locally, the ^{18}O enrichment in the Northern Component Water box is imported from the intermediate Atlantic box; the nitrate $\delta^{18}O$ of the two boxes is indistinguishable. The $\delta^{18}O$ elevation of the intermediate Atlantic, in turn, derives from partial nitrate consumption in the Subantarctic. Thus, in the model, the nitrate ^{18}O enrichment in North Atlantic-sourced deep water is actually derived from the Subantarctic, explaining the lack of a distinct North Atlantic end-member in the plots of nitrate $\delta^{18}O$ vs. regenerated/total $[PO_4^{3-}]$ (Figs. 4f and 5b).

3.1.2. *Mean ocean nitrate $\delta^{18}O$*

Nitrification and algal assimilation are not inputs or outputs of oceanic fixed N, but they are inputs and outputs of nitrate as an oxygen-bearing ion. Thus, for the model experiments including only internal N cycling, mean ocean nitrate $\delta^{18}O$ is set by a large scale steady state between nitrate addition by nitrification and the fractionating loss by algal assimilation, the latter elevating mean ocean nitrate $\delta^{18}O$ above its input value. If the assumed isotope effect of 5‰ for nitrate assimilation were completely expressed at the global ocean scale (e.g., as in the one box model, Fig. 1), mean ocean nitrate $\delta^{18}O$ in this simulation would be 5‰ higher than that of newly produced nitrate from nitrification. The actual model

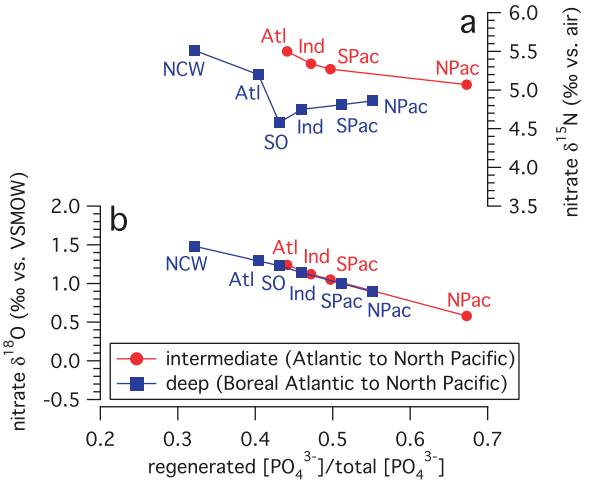

Fig. 5. For a slight variation of the model Southern Ocean nutrient field from the standard case, in which all of the Southern Ocean surface boxes are set to the same phosphate concentration (1.62 μmol/kg; as in Keir, (1988)), the nitrate $\delta^{15}N$ (a) and $\delta^{18}O$ (b) plotted versus the ratio of regenerated-to-total phosphate. As in Fig. 4, the red circles and blue squares indicate intermediate and deep boxes, respectively. In this case, as in the standard case, all O atoms in nitrate are derived from ambient water. Relative to Table 3, this is from experiment I.C.

output for mean ocean nitrate $\delta^{18}O$ is only ~1.1‰ higher than that of newly produced nitrate (Table 3). Thus, the nitrate assimilation isotope effect is expressed at the global scale at only one fifth its organism-scale value. In the low latitude surface, complete consumption prevents expression of the isotope effect (Fig. 2b). Because the North Atlantic surface nitrate assimilation rate is insignificant in the standard case of the model, North Atlantic surface nitrate assimilation plays little role in either the expression or under-expression of nitrate assimilation at the global scale. As verification of this, when North Atlantic surface nitrate assimilation is set to zero in the model, the mean ocean nitrate $\delta^{18}O$ does not change from the standard case value of 1.1‰ (experiment not shown). Thus, in the model, the partial nitrate assimilation in the Southern Ocean is essentially solely responsible for the ^{18}O enrichment of mean ocean nitrate relative to its nitrification input. Sensitivity tests of a similar type (not shown) suggest that, in the standard case, 85% (or 0.9‰) of the 1.1‰ mean ocean nitrate $\delta^{18}O$ elevation is due to the combined nitrate assimilation in the open Antarctic and Subantarctic Zones, which inject ^{18}O-enriched nitrate into the intermediate boxes. The remaining 0.2‰ is due to partial nitrate assimilation in the Polar Antarctic Zone.

3.1.3. *Nitrate $\delta^{15}N$*

At a given depth level, the $\delta^{15}N$ of nitrate also shows a generally negative correlation with total $[PO_4^{3-}]$ (Fig. 4a, filled symbols) and with the ratio of regenerated to total $[PO_4^{3-}]$ (Fig. 4e, filled symbols). Much as with the O isotopes, this correlation is due to partial assimilation in Southern Ocean surface boxes, the transport of partially consumed and thus isotopically enriched nitrate into the interior, and the subsequent addition of lower-$\delta^{15}N$ N from the regeneration of organic N export. However, the $\delta^{15}N$ difference between the intermediate and deep levels (with $\delta^{15}N$ being higher for a given ratio of regenerated to total $[PO_4^{3-}]$ at intermediate levels) is greater than the corresponding $\delta^{18}O$ difference. Moreover, in contrast to $\delta^{18}O$ (Fig. 5b), the elevation of intermediate-depth nitrate $\delta^{15}N$ over the deep ocean trend occurs even in the model with the uniform Southern Ocean nutrient field (Fig. 5a). These differences arise from the fact that the $\delta^{15}N$ of regenerated nitrate depends on the $\delta^{15}N$ of organic N being regenerated, while the $\delta^{18}O$ of newly regenerated nitrate does not. Nitrate is upwelled into the Southern Ocean surface, where it undergoes partial consumption. The low-$\delta^{15}N$ organic N from consumption in the Southern Ocean surface sinks into deep Southern Ocean water from which this N originally came, lowering the $\delta^{15}N$ of nitrate in this region of the ocean interior. The nitrate upwelled into the open AZ, elevated in $\delta^{15}N$ by the partial nitrate consumption there and the SAZ, is subducted into the low latitude intermediate boxes, effectively separating this high-$\delta^{15}N$ nitrate from the complementary low-$\delta^{15}N$ sinking N that results from partial nitrate consumption in the AZ and SAZ. In the low latitudes, nitrate upwelled into the surface yields sinking N with a $\delta^{15}N$ similar to that of the supply, the regeneration of which in the intermediate box lowers the $\delta^{18}O$ of nitrate but has little effect on its $\delta^{15}N$. As described above for the O isotopes, the high nitrate $\delta^{15}N$ of the deep high-latitude North Atlantic box is imported from the intermediate Atlantic box, which itself is ultimately derived from the Subantarctic Zone surface box (Fig. 3). It should be noted that the $\delta^{15}N$ of mean ocean nitrate is prescribed as 5.0‰ in these "closed system" experiments; all of the boxes of the "no assimilation fractionation" case collapse onto this value (Figs. 4a and e).

3.2. *The 'full' model including the ocean N budget*

3.2.1. *Mean ocean nitrate $\delta^{15}N$ and $\delta^{18}O$*

Mean ocean nitrate $\delta^{15}N$ in the standard case of the full model is 4.3‰ vs. air (Table 3). This value is lower than that of the real ocean, which, while imperfectly known, is close to 5‰ (Sigman et al., 2000). This value is controlled by the fixed N budget of the model, that is, the $\delta^{15}N$ of the N inputs (N_2 fixation only in this model) and losses (water column and sedimentary denitrification). With the global rates for these processes from our multi-box model (a water column-to-sedimentary denitrification rate ratio of 0.37 (Table 1)) and assuming a $\delta^{15}N$ of −1‰ for newly fixed N and isotope effects of 25‰ and 0‰ for water column and sedimentary denitrification, respectively), a 1-box model (Fig. 1a; as used in Brandes and Devol, 2002) predicts that the $\delta^{15}N$ of the ocean should be 5.8‰. The 1.5‰ difference from the multi-box result (4.3 vs. 5.8‰) indicates 22% isotopic under-expression of water column denitrification because of local nitrate depletion within suboxic zones (the "dilution effect" of Deutsch et al., 2004).

The $\delta^{18}O$ of mean ocean nitrate for this model case including N_2 fixation and denitrification is ~2.4‰ relative

to the nitrification source, and 1.4‰ if the isotope effect of nitrate assimilation is set to zero (Table 3). These values can be compared with expectations from the one-box steady state model of nitrate O isotopes (Fig. 1b). With water column denitrification, sedimentary denitrification, and nitrate assimilation occurring at our full model's rates (36.8, 99.1, and 512.0 Tg N yr^{-1}, respectively, Table 1) and assuming expressed O isotope effects of 25‰, 0‰, and 5‰ for the three processes, the one-box steady state model (Fig. 1b) would predict a mean nitrate $\delta^{18}O$ of 5.4‰ relative to the nitrification source. Taking into account the 22% dilution effect estimated from CYCLOPS, this value would be reduced to 4.2‰. If the isotope effect of nitrate assimilation is set to zero, this same calculation yields a $\delta^{18}O$ of 1.4‰ and 1.1‰, without and with the dilution effect consideration, respectively. Not surprisingly, our multi-box model prediction of 2.4‰ falls between these two end-member calculations from the one-box model, suggesting that the isotope effect of nitrate assimilation is expressed in the ocean interior at the level of 25 or 42%, without and with the dilution effect consideration, respectively. In summary, nitrate assimilation, the isotope effect of which is greatly under-expressed in the ocean interior, lowers the $\delta^{18}O$ of mean ocean nitrate from what one would expect if assimilation were presumed to express its full isotope effect on the global ocean or if nitrate assimilation were not included as a nitrate loss term. Since nitrate assimilation in the low-nutrient surface is mechanistically linked to nitrification in the subsurface, another way to describe the effect is that this nitrification "washes away" the deep nitrate ^{18}O enrichment associated with isotope fractionating nitrate loss.

3.2.2. *Inter-box variation in nitrate $\delta^{15}N$ and $\delta^{18}O$*

For both N and O isotopes and both deep and intermediate levels, the addition of the N budget only subtly affects vertical and lateral gradients from the North Atlantic through the Southern Ocean to the Indian. The main changes occur in the lateral gradients in nitrate $\delta^{15}N$ and $\delta^{18}O$ from the Indian to the North Pacific and in the vertical gradients within the Pacific (Fig. 6a, b, e, f). Because of water column denitrification, which occurs predominantly in the North Pacific and at intermediate depth in the model, nitrate $\delta^{15}N$ and $\delta^{18}O$ increase from the Indian Ocean to the North Pacific, especially at intermediate depth. The boxes can be grouped along branches of the subsurface circulation: the North Atlantic-Atlantic-Southern Ocean-Indian (NA-A-SO-I) deep transect, the Indian-South Pacific-North Pacific (I-SP-NP) deep transect, the Atlantic-Indian (A-I) intermediate transect, and the Indian-South Pacific-North Pacific intermediate transect. In the case of the NA-SO-I deep transect and the A-I intermediate transect, the decrease in both nitrate $\delta^{15}N$ and $\delta^{18}O$ from NA (or A) to I is due to regeneration and nitrate production (see Section 3.1.). In the I-SP-NP transects, $\delta^{15}N$ and $\delta^{18}O$ increase due to denitrification.

There is strong covariation between nitrate $\delta^{18}O$ and $\delta^{15}N$ throughout the subsurface, with a ratio of $\delta^{18}O$-to-$\delta^{15}N$ variation ("$\Delta\delta^{18}O/\Delta\delta^{15}N$") that is significantly less than 1 (Fig. 7a, filled symbols). Focusing on the boxes most strongly affected by denitrification, the ratio of $\Delta\delta^{18}O/\Delta\delta^{15}N$ from the I-SP-NP transect is 0.54 ± 0.002 ($\pm$2SD) for the deep boxes, 0.71 ± 0.04 for the intermediate boxes, and 0.68 ± 0.04 taking intermediate and deep boxes together. The model imposes equal-amplitude N and O isotope effects for both denitrification and nitrate

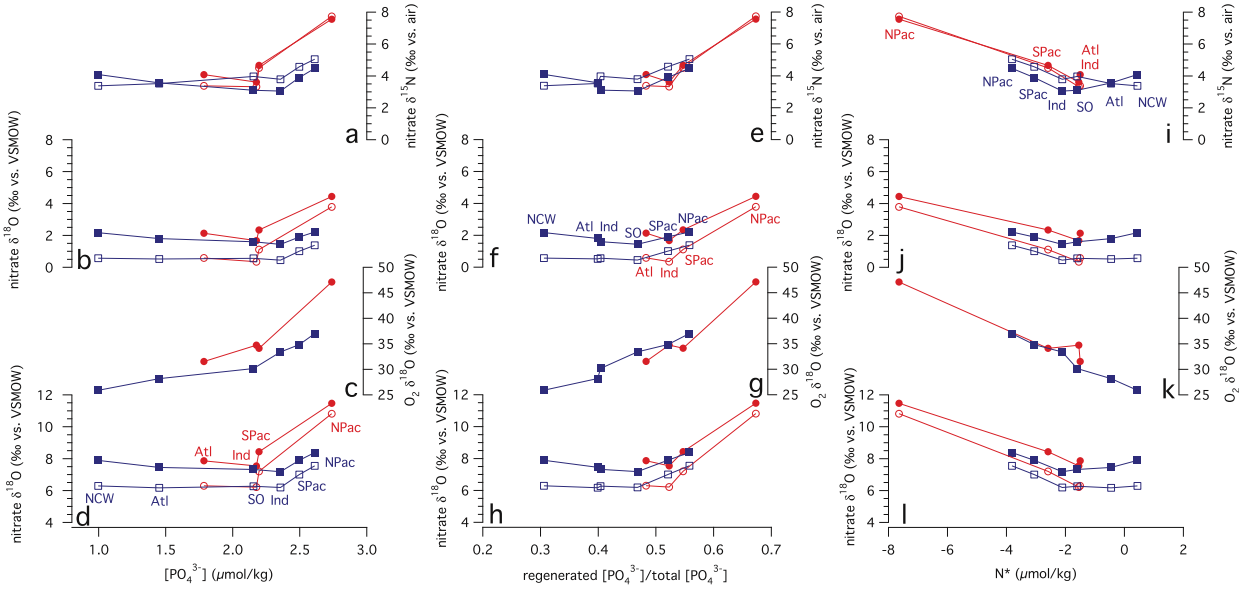

Fig. 6. For the version of the model including the oceanic N budget (N_2 fixation and denitrification), model output for subsurface box nitrate $\delta^{15}N$ (a, e, i), nitrate $\delta^{18}O$ (b, f, j; d, h, l), and O_2 $\delta^{18}O$ (c, g, k). Figure symbols and panels are as in Fig. 4 for the model without the N budget; the sole change is that a column of plots are added to the right (i – l) where the isotopic parameters are plotted against N* ($N^* = [NO_3^-]-16^*[PO_4^{3-}]+2.9$, in μmol/kg (Deutsch et al., 2001)). Relative to Table 3, the filled symbols in (a, b, e, f, i, j) are from experiment II.A., while the open symbols in (a, b, e, f, i, j) are from II.B.. The filled symbols in (d, h, l) are from experiment II.C., while the open symbols in (d, h, l) are from II.D.

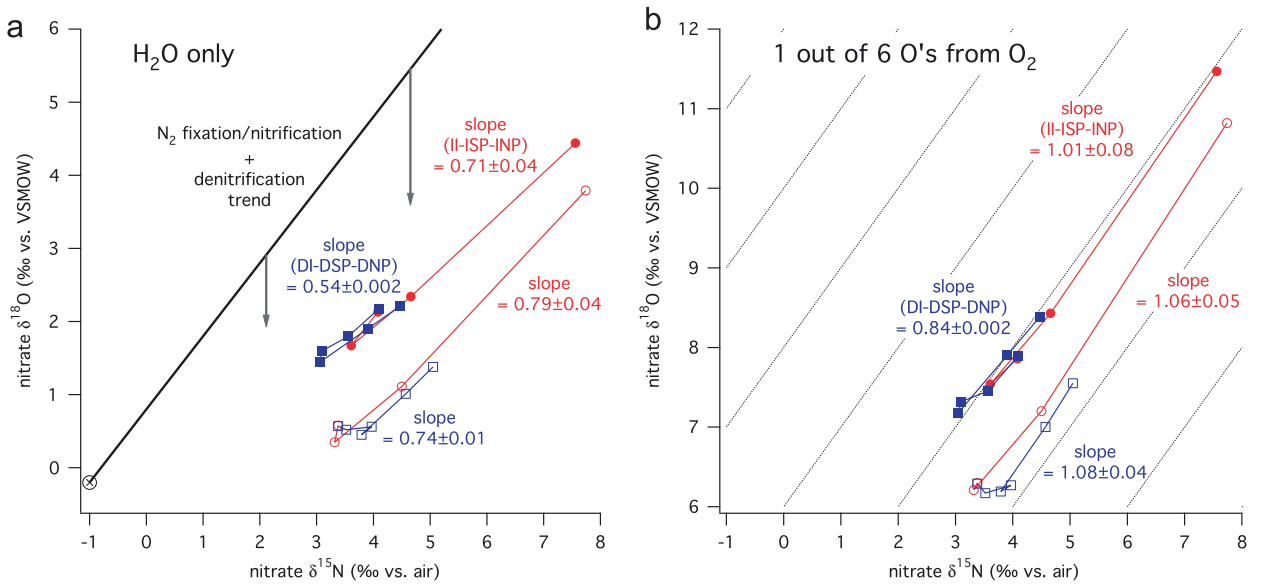

Fig. 7. For the version of the model including the oceanic N budget, subsurface box nitrate $\delta^{18}O$ versus nitrate $\delta^{15}N$. Figure symbols and connecting lines are as in Figs. 4–6. (a) shows model cases where all O atoms in nitrate are inherited from ambient water, while (b) shows model cases were one out of six oxygen atoms is inherited from ambient dissolved O_2. Relative to Table 3, in (a), the filled symbols are from experiment II.A., while the open symbols are from II.B.. In (b), the filled symbols are from experiment II.C., while the open symbols are from II.D.. Calculated slopes are for the Indian-South Pacific-North Pacific transects, separately for intermediate and deep levels; uncertainties are ±2SD (i.e. 95% confidence). In (a), the circled x in the lower left indicates the estimated $\delta^{15}N$ and $\delta^{18}O$ of nitrate deriving from N_2 fixation, and the bold black line shows the expected 1:1 correlation between nitrate $\delta^{18}O$ and $\delta^{15}N$ in a hypothetical ocean that included only N_2 fixation (followed by nitrification) and denitrification. The gray arrows then indicate the qualitative effect of including nitrate assimilation in the low latitude surface ocean coupled to N export and nitrification in the ocean interior. In (b), the background lines have a slope of 1.

assimilation. Thus, the deviation from 1:1 variation is of interest.

A reasonable hypothesis for the deviation of $\Delta\delta^{18}O/\Delta\delta^{15}N$ from 1 is that combining the preformed/regenerated nutrient dynamic with the denitrification dynamic has a canceling effect on O isotope variation that is greater than any such effect on the N isotopes. An increasing fraction of regenerated nutrients from the deep Indian through the deep North Pacific causes nitrate $\delta^{18}O$ (but not $\delta^{15}N$) to decrease in the model lacking the N budget components (Fig. 4a, b, e, f), while denitrification causes both $\delta^{18}O$ and $\delta^{15}N$ to increase into the deep North Pacific (Fig. 6 b, f), qualitatively justifying this hypothesis. In the "no assimilation fractionation" case (II.B), which lacks the preformed/regenenerated nitrate isotope dynamic, $\delta^{18}O$-to-$\delta^{15}N$ trends for the I-SP-NP transects have slopes of 0.79±0.02 and 0.74±0.01 for intermediate and deep levels, respectively (±2SD; Fig. 7a, red and blue open symbols), compared with slopes of 0.71 and 0.54 for the I-SP-NP transect (intermediate and deep) in the standard case output from the model (filled symbols). Consistent with the closed system experiments (Fig. 4), the comparison in Fig. 7a indicates that isotope dynamics arising from partial nitrate assimilation in the polar boxes drives a coherent elevation in intermediate box $\delta^{15}N$ and $\delta^{18}O$ relative to the deep boxes, with the effect on the intermediate-deep difference being greater for $\delta^{15}N$ than $\delta^{18}O$. In any case, it appears that the preformed/regenerated nitrate dynamic explains less than half of the deviation from unity in the $\Delta\delta^{18}O/\Delta\delta^{15}N$ observed in the I-SP-NP intermediate and deep transects.

The deviation from unity in the $\Delta\delta^{18}O/\Delta\delta^{15}N$ largely derives from the interaction between the N budget (N_2 fixation and denitrification) and the internal cycling of N in the low latitude ocean (nitrate assimilation and regeneration/nitrification). Given only N_2 fixation (with nitrification to nitrate) and denitrification operating in the ocean N cycle, one would expect equivalent increases in nitrate $\delta^{18}O$ and $\delta^{15}N$ from regions of (net) N_2 fixation to regions of (net) denitrification. In a plot of nitrate $\delta^{18}O$ vs. $\delta^{15}N$, this behavior would define a straight line with a slope of 1 (bold black line in Fig. 7a), originating from the $\delta^{18}O$ of nitrification and the $\delta^{15}N$ of N_2 fixation (circled X in Fig. 7a). However, subsurface nitrate is being supplied continuously to the surface ocean, driving N export that is ultimately regenerated back to nitrate in the subsurface. This cycle of supply, export, and regeneration preserves the $\delta^{15}N$ of the nitrate cycled through it and can work to communicate a $\delta^{15}N$ signal beyond its source region: sinking N from ^{15}N-enriched nitrate can transport the ^{15}N signal into deeper waters, such that its remineralization works to diffuse the elevated nitrate $\delta^{15}N$ over a larger volume of the ocean interior. In contrast, this cycle will continuously force the $\delta^{18}O$ of subsurface nitrate toward the $\delta^{18}O$ of newly nitrified nitrate. Not only will this reduce the $\delta^{18}O$ of mean ocean nitrate (as described in Section 3.2.1.), but it will also dampen the denitrification-driven $\delta^{18}O$ gradients within the ocean interior (gray arrows in Fig. 7a). The latter effect explains the model

observation that the $\Delta\delta^{18}O/\Delta\delta^{15}N$ is less than 1. Consistent with this explanation, the model's $\Delta\delta^{18}O/\Delta\delta^{15}N$ decreases further (deviates further from 1) as water column denitrification is slowed while the rate of internal N cycling is held constant (results not shown).

Above, we described that part of the $\Delta\delta^{18}O/\Delta\delta^{15}N$ deviation from 1 derives from the destructive interference of the nitrate $\delta^{18}O$ gradients generated by denitrification and partial nitrate assimilation. We can now see that there is a better way to describe the role of partial nitrate assimilation in generating a $\Delta\delta^{18}O/\Delta\delta^{15}N$ below 1 (Sigman et al., 2009). Like denitrification, partial nitrate assimilation drives nitrate $\delta^{15}N$ and $\delta^{18}O$ elevation in some ocean interior boxes. The sequence of low latitude (complete) nitrate assimilation, sinking N, and regeneration preferentially removes $\delta^{18}O$ elevation, be it from denitrification or partial nitrate assimilation, lowering the $\Delta\delta^{18}O/\Delta\delta^{15}N$ below 1. Thus, the $\Delta\delta^{18}O/\Delta\delta^{15}N$ deviation from 1 is attributed to the interaction of low latitude N cycling with both denitrification and high latitude partial nitrate assimilation.

3.2.3. *A case with O_2 incorporation into nitrate*

The main change in this case from the standard case above is in the lateral gradients at both intermediate and deep levels as one goes from the Southern Ocean and Indian northward through the Pacific, along which the denitrification signal in $\delta^{15}N$ and $\delta^{18}O$ is important. Relative to the standard case, the nitrate $\delta^{18}O$ increase into the North Pacific is greater because, along this path, O_2 consumption and thus O_2 $\delta^{18}O$ increase, such that the $\delta^{18}O$ of nitrate produced from nitrification increases into the North Pacific. This causes nitrification to be less effective at erasing the denitrification-driven elevation in $\delta^{18}O$. The greater $\delta^{18}O$ increase leads to a $\Delta\delta^{18}O/\Delta\delta^{15}N$ close to 1 (Fig. 7b, filled symbols).

4. Model/data comparison

Below, the model results are compared with data from a set of water column profiles from the global ocean (Table 2; Fig. A1). This comparison is separated into two components: (1) isotopic gradients, and (2) the mean ocean isotopic composition. Because gradients associated with both the ocean's N budget (N_2 fixation and denitrification) and its internal N cycle (nitrate assimilation and regeneration/nitrification) are apparent in the model, we separate the discussion of gradients into these components.

4.1. *Isotopic gradients*

4.1.1. *Isotopic gradients from denitrification and N_2 fixation*

From the Southern Ocean and Indian to the North Pacific, the model output including the N budget shows increases in nitrate $\delta^{15}N$ and $\delta^{18}O$ that coincide with a decrease in N*, a measure of the excess or deficit of nitrate relative to the mean ocean relationship with phosphate ($N^* = [NO_3^-]-16^*[PO_4^{3-}]+2.9$ (in $\mu mol\,kg^{-1}$) (Deutsch et al., 2001)). This signal is most prominent in the intermediate boxes, but the deep boxes also show the pattern, with $\delta^{15}N$ increasing by ~1.7‰ from the deep Indian to deep North Pacific. In nitrate isotope data from deep waters (below 1500 m), the increases in $\delta^{15}N$ and $\delta^{18}O$ with decreasing N* are much weaker than in the model (Fig. 8c and d). One possible explanation is that this results from sedimentary denitrification, which lacks a large isotope effect. Indeed, the lowest-N* deep point is from the Bering Sea, where a deeply focused nitrate deficit and a lack of nitrate heavy isotope enrichment argue for sedimentary denitrification (Lehmann et al., 2005). As explained above, the model's deep ocean $\delta^{15}N$ gradient from the Southern Ocean and Indian to the North Pacific is also enhanced by low-$\delta^{15}N$ sinking N from partial nitrate assimilation in the Southern Ocean surface boxes, which is regenerated in the model's deep Southern Ocean, lowering its nitrate $\delta^{15}N$; this is discussed in the next section.

In comparing the gradients in $\delta^{15}N$ and $\delta^{18}O$, we first neglect the data point that derives from the denitrification zone off the coast of Baja California (Fig. 9, dashed line leading off the plot labeled ETNP). Having done so, while the data uncertainties are considerable at the relevant scale, the data appear to support the model finding that the $\Delta\delta^{18}O/\Delta\delta^{15}N$ ratio of the trend from the North Atlantic to the North Pacific is less than the value of 1 imposed by denitrification alone (Figs. 7 and 9). While the calculated $\Delta\delta^{18}O/\Delta\delta^{15}N$ slopes are uncertain, they all fall below 1 (see Fig. 9 caption). Moreover, focusing on 200–400 m thermocline water from the North Atlantic profile, which has a significant portion of nitrate from newly fixed N (Knapp et al., 2008), its nitrate has a ~2‰ lower $\delta^{15}N$ than the intermediate and deep profile averages but a similar $\delta^{18}O$ (Fig. 9, purple asterisk). This corroborates the sense of weaker variations in $\delta^{18}O$ than in $\delta^{15}N$ within the ocean interior. In the model, the $\Delta\delta^{18}O/\Delta\delta^{15}N$ below 1 in the interior is attributed to low latitude nitrate assimilation followed by sinking of organic N and its regeneration/nitrification at depth. The data in Fig. 9 suggest that this is also important in the real ocean (Sigman et al., 2009).

The low-O_2 mid-depth waters off the coast of Baja contain nitrate that has more enrichment in ^{18}O than in ^{15}N, relative to either the deep or intermediate-depth open North Pacific (Fig. 9, falling off the plot and indicated by the arrow labeled 'ETNP'). This is in the opposite sense of the $\Delta\delta^{18}O/\Delta\delta^{15}N$ ratio deviation from 1 that we have just described for the model and for open North Pacific data. In previous work (Sigman et al., 2005), we described the structure of this deviation in detail and put forward two explanations for its existence. One of these explanations involves the regeneration of newly fixed N, which would lower the $\delta^{15}N$ of nitrate more than it would lower its $\delta^{18}O$ if it occurs in waters that are proximal to the denitrification zone. A view of that explanation in the context of the current global analysis is that the suboxic zones may be regions where the rate of the denitrification/N_2 fixation couple approaches that of the nitrate assimilation/nitrification cycle. In this case, subsurface nitrate should converge toward equivalent denitrification-driven ^{18}O and ^{15}N enrichments, relative to the $\delta^{18}O$ of nitrification and the $\delta^{15}N$ of N_2 fixation, respectively (i.e. the bold trend in Fig. 7a). Such equivalent ^{18}O and ^{15}N

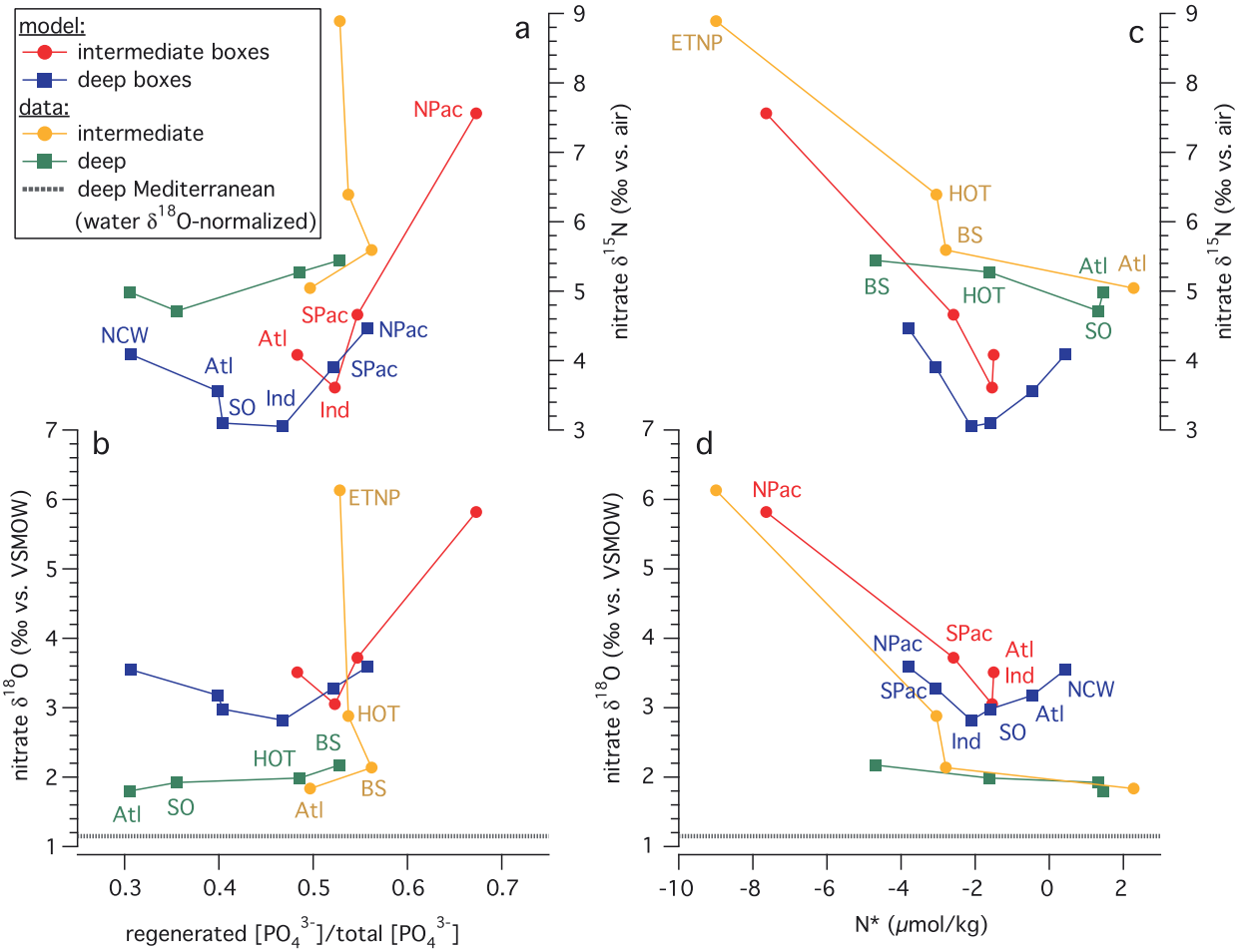

Fig. 8. Comparison of model and data for nitrate $\delta^{15}N$ (a, c) and $\delta^{18}O$ (b, d) versus the ratio of regenerated to total phosphate (a, b) and versus N* (c, d). The model output shown are from the standard case of the model including the ocean N budget (II.A. from Table 3); red circles denote intermediate boxes, and blue squares denote deep boxes. The data are shown in orange circles (intermediate) and green squares (deep). The deep points are connected by line following the sequence: North Atlantic – Southern Ocean – North Pacific – Bering Sea. The intermediate points are connected by line following the sequence: North Atlantic – Bering Sea – North Pacific– Eastern Tropical North Pacific; the order of the Bering Sea and North Pacific points have been reversed here to address hydrographic proximity to the ETNP. Values are $[NO_3^-]$- and depth interval-weighted averages (intermediate: 300 – 1500 m; deep: 1500 m-bottom). Our preliminary estimate of 1.15‰ for the $\delta^{18}O$ of nitrification in water identical to VSMOW is plotted as a dashed line across (b) and (d), and the model nitrate $\delta^{18}O$ is plotted assuming this offset as well (keeping in mind that the mean $\delta^{18}O$ of seawater in the model is ~ -0.2‰ vs. VSMOW). (For interpretation of the references to colour in this figure legend, the reader is referred to the web version of this article.)

enrichment in the region of the denitrification zone would appear as a $\Delta\delta^{18}O/\Delta\delta^{15}N > 1$ when comparing the region's nitrate to mean ocean nitrate (trend toward ETNP in Fig. 9), because mean ocean nitrate is depressed in $\delta^{18}O$ (but not in $\delta^{15}N$) by the low latitude nitrate assimilation/nitrification cycle.

As described above, one critical uncertainty in the nitrate isotopes is the degree to which O_2 contributes O atoms to nitrate during nitrification. Mechanistic studies indicate that the fraction of O atoms from O_2 is not more than 1 in 3 and may be much less than this ratio (Casciotti et al., 2002, and references therein). In the "O_2 influence" model experiment, in which O_2 is incorporated into nitrate at a level of 1 in 6 O atoms, the model would predict a nitrate $\delta^{18}O$ increase into the North Pacific that is equivalent to the $\delta^{15}N$ increase (a $\Delta\delta^{18}O/\Delta\delta^{15}N$ near 1; Fig. 7b). This does not appear to match the observations. Workers in the terrestrial biogeochemistry community, based on their reading of the biochemical literature, have tended to assume that 1/3 of O's in nitrate derive from O_2 (Böhlke et al., 1997; Kendall, 1998). If this ratio is used in the model, the DI-DSP-DNP and II-ISP-INP transects yield $\Delta\delta^{18}O/\Delta\delta^{15}N$ of 1.14 ± 0.0004 and 1.31 ± 0.12, respectively (± 2SD, results not shown); these ratios are even less consistent with the oceanographic data. With the caveat that future work may uncover aspects of nitrate O isotope systematics not considered here, the model/data comparison would seem to argue against even minor amounts of O_2 being incorporated into deep ocean nitrate.

4.1.2. *Isotopic gradients from algal nitrate assimilation and nitrification*

As found from previous measurements (Sigman et al., 2000), basin-averaged deep nitrate $\delta^{15}N$ varies little

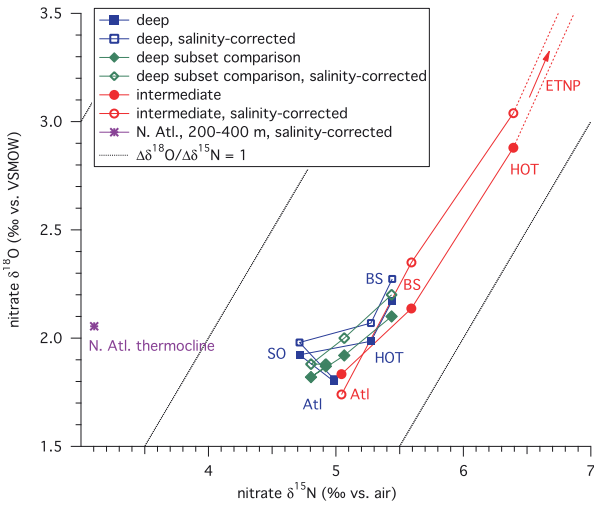

Fig. 9. Station averages for nitrate isotope data from deep and intermediate-depth levels, plotted in nitrate $\delta^{18}O/\delta^{15}N$ space. Red circles and blue squares indicate intermediate and deep levels, respectively. Open symbols show the salinity- (water $\delta^{18}O$-) normalized nitrate $\delta^{18}O$ measurements. The intermediate and deep data are connected by lines as in Fig. 8. The HOT-to-ETNP trend is indicated by the dashed line. The green diamonds indicate the results for the "deep subset" comparison, a set of deep samples taken from each of the profiles and analyzed within the same analysis runs (Table 2; Appendix B). Intended to address the small amplitude of deep ocean isotope variations, these data provide the best measure of the $\delta^{18}O$-to-$\delta^{15}N$ relationship of global isotopic variations in deep nitrate, but they come from only a portion of each depth profile and thus do not cover an identical isotope range as the profile averages. Uncertainties, while not plotted, are significant at this scale; for the "deep subset" data, the 95% confidence intervals for nitrate $\delta^{18}O$ and $\delta^{15}N$ are estimated to be ± 0.3 and ± 0.1‰, respectively. Nevertheless, all statistical regressions indicate a $\Delta\delta^{18}O/\Delta\delta^{15}N$ ratio of less than 1 (deep subset comparison: 0.44 ± 0.04 and 0.52 ± 0.19; profile deep data: 0.49 ± 0.50 and 0.69 ± 0.86; profile intermediate data: 0.79 ± 0.21 and 0.9 ± 0.14; based on model-II least squares regression, ± 2SD, the latter value in each pair being for the salinity-corrected $\delta^{18}O$ data).

(by ~0.5‰) among open ocean basins, around a mean of ~5‰ (Fig. 8 a, green squares; Fig. 9, blue squares and green diamonds). In contrast, in both versions of the model (with and without the N budget), there is a ~1‰ decrease in $\delta^{15}N$ from the high latitude North Atlantic to the Southern Ocean (Figs. 4, 6 and 8). This is associated with an increase in the regenerated to total nutrient ratio heading southward and is largely due to the regeneration of low-$\delta^{15}N$ sinking N in the deep Southern Ocean, with the partially consumed (and thus high-$\delta^{15}N$) nitrate in the Southern Ocean surface layer being exported to the intermediate boxes. There is perhaps a hint of such a North Atlantic-to-Antarctic $\delta^{15}N$ decrease in the deep ocean data, but it is $\leq$0.3‰ (Figs. 8a and c). A previous deep basin comparison indicated no measurable $\delta^{15}N$ difference between the deep North Atlantic and the deep Southern Ocean (Sigman et al., 2000). Taken together, the available data indicate that the model's preformed/regenerated nitrate-driven N isotope signal in the deep ocean is too great.

A similar story is told by the gradients in the $\delta^{18}O$ of nitrate. Due to regeneration, the standard model case produces a ~0.7‰ decrease from the North Atlantic to the Southern Ocean. The data do not support such a difference (Table 2; Fig. 8). A plausible explanation for this lack of nitrate $\delta^{15}N$ and $\delta^{18}O$ decrease from the Atlantic to the Antarctic is that Atlantic ^{15}N and ^{18}O enrichment due to partial nitrate assimilation is offset by ^{15}N and ^{18}O enrichment in the Antarctic from communication with the Indo-Pacific, which hosts denitrification. However, the similar values for N* for our North Atlantic and Antarctic profiles argue against this (Fig. 8). Thus, an explanation is required.

4.2. Mean ocean nitrate $\delta^{18}O$

Given knowledge of the $\delta^{18}O$ of newly formed nitrate, the model/data comparison of mean ocean nitrate $\delta^{18}O$ become an important constraint. The Mediterranean Sea data are potentially helpful in this regard. Calculations indicate that all nitrate in the deep Mediterranean is from regeneration (Fig. A1b), and water column denitrification is not occurring at significant rates within the basin. So it should have minimal nitrate ^{18}O enrichment from nitrate assimilation or denitrification and should, therefore, indicate the $\delta^{18}O$ of nitrate newly produced from nitrification. This use of the Mediterranean data cannot be completely valid, as there seem to be isotopic variations within the deep Mediterranean, in particular, an increase in $\delta^{18}O$ near the base of the profile (Fig. A1d and e); nevertheless, it is a reasonable assumption until stronger constraints are available.

The $\delta^{18}O$ of nitrate in the deep Mediterranean Sea is $\leq$1‰ higher than in the global deep ocean. However, the $\delta^{18}O$ of seawater in the Mediterranean is high, complicating this comparison. Accounting for this, global deep ocean nitrate $\delta^{18}O$ appears to be $\leq$1‰ greater than the $\delta^{18}O$ of nitrification (Fig. 8b, d), the latter being 1.15‰ higher than ambient seawater according to the Mediterranean data (see Appendix B; see also Casciotti et al., 2008). The model's standard case with and without the N budget predict a mean ocean nitrate $\delta^{18}O$ that is 2.4‰ and 1.1‰ greater than the nitrification source, respectively. Thus, while the model predicts that ocean nitrate $\delta^{18}O$ will be minimally elevated relative to its nitrification source, the data suggest even less ^{18}O enrichment than the model. Just as measured nitrate $\delta^{18}O$ gradients are weaker than predicted by the model, mean ocean nitrate $\delta^{18}O$ is closer to its apparent nitrification source than predicted by the model.

The model's mean ocean nitrate $\delta^{15}N$ appears to be ~0.7‰ lower than in the real ocean (Fig. 8). As discussed above, this discrepancy may involve the net isotope discrimination by the combined water column and sedimentary denitrification of the ocean (Deutsch et al., 2004). If so, the model should also tend to underestimate the $\delta^{18}O$ of oceanic nitrate, although to a lesser degree because denitrification is only one of the two sinks for nitrate O atoms in the model, nitrate assimilation being the other. Whatever process causes the model to overestimate mean ocean nitrate $\delta^{18}O$, it must overwhelm this effect.

4.3. Implications of the model/data discrepancies

Why does nitrate $\delta^{18}O$ in the ocean vary less among basins and with depth than predicted by the model, and why does it appear that mean ocean nitrate $\delta^{18}O$ is so close to its nitrification source? The processes that the model has highlighted as muting nitrate $\delta^{18}O$ variations in the interior and lowering its mean value may be even more important in the real ocean than they are in the model. One ocean process, or condition, that reduces gradients in both the $\delta^{18}O$ and $\delta^{15}N$ of nitrate (as well reducing the $\delta^{18}O$ of mean ocean nitrate) is the tendency for either insignificant or complete nitrate consumption in most of the surface ocean, with few domains (e.g., the Subantarctic) of intermediate nitrate consumption (DiFiore et al., 2006; Sigman et al., 2000). To the degree that the data show weaker gradients than the model for both $\delta^{18}O$ and $\delta^{15}N$ of nitrate, under-representation of this global ocean characteristic by the model is a plausible explanation for the evidence that the model over-predicts the $\delta^{18}O$ of mean ocean nitrate.

We have also recognized processes that alter solely the O isotopes of nitrate. Supply and uptake of nitrate in the nutrient-poor surface ocean followed by sinking and regeneration in the ocean interior will reset subsurface nitrate $\delta^{18}O$ to its nitrification value while having no major impact on nitrate $\delta^{15}N$. Nitrate that has previously been enriched in $\delta^{18}O$ by either partial nitrate assimilation or denitrification is reset toward the $\delta^{18}O$ of nitrification. Thus, to the degree that the model/data discrepancy in gradients and mean ocean values is greater for nitrate $\delta^{18}O$ than for $\delta^{15}N$, nitrate cycling in the nutrient-poor ocean that is faster in the real ocean than in the model is a plausible explanation.

At this point, the nitrate isotope data do not allow for a clear distinction between these two possible model errors: (1) over-representation of high latitude partial nitrate assimilation, or (2) under-representation of low latitude nitrate assimilation/nitrification cycling. Indeed, we suspect that both are involved. It can be said that the data shown here offer some support for the first source of error. In the model, as described above, high-$\delta^{15}N$ and -$\delta^{18}O$ nitrate formed in the Subantarctic travels across through the intermediate boxes to yield North Atlantic Deep Water with a preformed nitrate with both high $\delta^{15}N$ and high $\delta^{18}O$. Given that the deep North Atlantic data do not show this elevation in either $\delta^{15}N$ or $\delta^{18}O$, we infer that the model does indeed overestimate the impact of partial nitrate assimilation in subpolar waters such as the Subantarctic on the $\delta^{15}N$ and $\delta^{18}O$ of nitrate in the mid-depth interior. We suspect that this involves the restriction of Subantarctic Mode Water and Antarctic Intermediate Water formation to the winter, when Southern Ocean nutrient consumption is weakest (DiFiore et al., 2006).

However, an argument can also be made that the model underestimates the impact of the low latitude N cycle on mid-depth nitrate $\delta^{18}O$. The fraction of major nutrient in the intermediate Atlantic that is preformed in the model is 0.5, and this is the dominant source of preformed nitrate for North Atlantic Deep Water. However, waters above ~600 m in the subtropical North Atlantic tend to have a smaller fraction of preformed nutrients than this (Fig. A1). This implies that nitrate in the intermediate water traveling northward in the Atlantic has been intensively cycled through the low-nutrient Atlantic surface (e.g., Jenkins and Doney, 2003), which would lead to lower nitrate $\delta^{18}O$ in the real intermediate-depth Atlantic. This, in turn, would yield a lower $\delta^{18}O$ for the nitrate fed into the deep Atlantic by North Atlantic Deep Water formation. Therefore, more active low latitude nitrate cycling in the real ocean than in the model, which seems plausible given known box model biases (Matsumoto et al., 2002), may help to explain the apparent over-prediction of mean ocean nitrate $\delta^{18}O$ by the model.

5. Conclusions

The N isotopes of nitrate provide an important constraint on the relative importance of water column and sedimentary denitrification in the global ocean's input/output budget of fixed N (Brandes and Devol, 2002; Deutsch et al., 2004). The O isotopes of nitrate add the potential to constrain the rate of internal nitrate cycling (nitrate assimilation and nitrification) relative to that of N budget processes. The nitrate O isotopes are also sensitive to the importance of partial nitrate assimilation, as occurs in high latitude regions, relative to complete nitrate assimilation, as occurs in the low latitude ocean; this can yield a deeper understanding of the origin of preformed nitrate in the ocean interior and also provides a target for biogeochemical models.

The model predicts that the $\delta^{18}O$ of mean ocean nitrate is only 2.4‰ higher than its source signal, with the ^{18}O enrichment being due roughly equally to denitrification and nitrate assimilation. This small amplitude of ^{18}O enrichment is driven by two dynamics. First, the isotope effect of nitrate assimilation in the model is very poorly expressed on the global scale because nitrate assimilation in the surface either is minimal (e.g., in the polar Antarctic) or goes to near-completion (e.g., in the subtropical ocean). This dynamic also leads to weak ocean gradients for both the $\delta^{18}O$ and $\delta^{15}N$ of nitrate. Second, the low latitude cycle of nitrate assimilation, sinking and nitrification works against the tendency of denitrification and high latitude partial nitrate assimilation to raise mean ocean nitrate $\delta^{18}O$ by replacing ^{18}O-enriched nitrate with newly nitrified nitrate. This process also works to weaken nitrate $\delta^{18}O$ gradients in the ocean, and it does so without having a similar impact on the gradients in nitrate $\delta^{15}N$.

A preliminary comparison with data from different regions of the global ocean confirms several aspects of the model. First, the lack of large, clear trends in either the N or O isotopes from the North Atlantic to the Southern Ocean are consistent with the N and O isotope effects of nitrate assimilation in the surface ocean having very modest impacts on deep ocean nitrate isotopes (see also' Sigman et al., 2000). Second, the ratio of $\delta^{18}O$ and $\delta^{15}N$ variation in the ocean interior appears to be less than 1, as predicted by the standard case of the model, confirming

that the O isotope signals of denitrification and partial nitrate assimilation are partially erased by nitrate cycling through the low latitude surface ocean, in which the nitrification component of this cycling "washes away" the ^{18}O enrichment. This process also lowers mean ocean nitrate $\delta^{18}O$ toward the value for nitrification, which is at least qualitatively apparent in both the model and the data. Finally, the model/data comparison seems to confirm that the contribution to O atoms in nitrate from O_2 is less than 1 out of 6, an upper limit on this contribution suggested by Casciotti et al. (2002). In the case of 1 or more out 6 oxygens coming from O_2, the model predicts that the O isotope variations would be nearly equivalent to the N isotope variations of nitrate in the ocean interior, apparently at odds with the data.

At the same time, these key observations from the model tend to be more pronounced in the data. The model predicts a ~0.9‰ decrease in nitrate $\delta^{15}N$ and a ~0.3‰ decrease in nitrate $\delta^{18}O$ from the deep Atlantic to the Southern Ocean, whereas the data fail to discern robust differences in $\delta^{15}N$ and $\delta^{18}O$ between these two regions. Thus, it would appear that the interior of the real ocean has weaker nitrate isotopic gradients from nitrate assimilation than does the model, and the model's gradients are themselves very weak. Moreover, if deep Mediterranean water is used as an indication of the $\delta^{18}O$ of newly produced (nitrified) nitrate relative to ambient water, then the deep ocean nitrate $\delta^{18}O$ is $\leq$1‰ higher than this value, less than half of the ^{18}O enrichment predicted by the model. This further suggests that the O isotopic impacts of nitrate assimilation and denitrification on mean ocean nitrate are even weaker than predicted by the model.

These results have implications for our understanding of the ocean's biological pump. The global efficiency of this pump can be framed in terms of the fraction of "major nutrient" (i.e. nitrate or phosphate) in the ocean interior that is regenerated (entering the interior as organic matter) as opposed to preformed (entering as unused nutrient that is mixed or advected into the interior). The greater the regenerated-to-total nutrient ratio, the greater the efficiency of the biological pump, and thus the more respired CO_2 that is sequestered in the interior (Ito and Follows, 2005; Sigman and Haug, 2003; Toggweiler et al., 2003). In the modern ocean, the concentrations of preformed and regenerated nutrients are similar in the deep waters of both the Atlantic and the Pacific (~2:1 in the North Atlantic, ~1:1 in the North Pacific), suggesting that the polar regions feeding water into the ocean interior have intermediate degrees of major nutrient consumption. However, the nitrate isotope model and its comparison with the data reveal that the similar concentrations of preformed and regenerated nutrients in the deep ocean arise instead from the degree to which low latitude, nutrient-poor surface waters are incorporated into new deep waters. That is, deep water masses are formed from a combination of very different surface waters, including both polar waters that have undergone nearly no major nutrient consumption and low latitude waters that have undergone nearly complete consumption.

The Polar Frontal and Subantarctic Zones in the modern Southern Ocean play an important role in ventilating the global intermediate ocean and thermocline, and this appears to be a region where partially consumed nitrate should be entering the ocean interior. In the model, the Subantarctic is responsible for most of the assimilation-driven ^{15}N and ^{18}O enrichment that enters the ocean interior. The isotope data appear to indicate that not much of this enrichment survives into the North Atlantic to be folded into the deep ocean as North Atlantic Deep Water. Given the data that we report here, we cannot yet say whether this is equally true for N and O. If it is true for both isotope systems, then the model/data comparison suggests a model/real ocean discrepancy in the nutrient content of newly forming subsurface waters, which requires consideration of the processes that inject new Antarctic Intermediate Water and Subantarctic Mode Water into the subsurface in the Southern Ocean. If further data demonstrate that the assimilation signal is weaker for the O isotopes than the N isotopes of nitrate, then this would implicate the low latitude N cycle: upward mixing and algal consumption in the photic zone, followed by regeneration/nitrification, converts preformed nitrate to regenerated nitrate, which would remove any ^{18}O enrichment from the nitrate. This process could erase the O isotope signal of partial nitrate consumption from thermocline and intermediate waters as these waters pass through the low latitudes, to a greater degree in the real ocean than in our model.

Acknowledgements

We thank G. Cane and R. Ho for isotope analyses, K. Casciotti for discussions, and two anonymous reviewers as well as the editors (M. Bacon, T. Trull) for their efforts to improve the manuscript. This work was supported by the US NSF through grants OCE-0447570 (D. M. S.), OCE-0550771 (C. D.), OCE-0326616 (D. M. K.), and EF-04245599 (D. M. K.), by the Gordon and Betty Moore Foundation (D. M. K.), and by the Deutsche Forschungsgemeinschaft (M. P. H., through G. H. Haug).

Appendix A. Model parameterizations of denitrification

A.1. Water column denitrification parameterization

There is the potential for a denitrification zone within each box of the model. The "oxygen minimum zone" (OMZ) is an ellipsoid volume with a horizontal long axis. Nested within the OMZ is a second ellipsoid representing the suboxic zone (SZ), in which denitrification occurs. The total volume of the OMZ is a function of the mean $[O_2]$ of the entire box, increasing dynamically as $[O_2]$ decreases. The volume of SZ as a proportion of OMZ is a function of the $[O_2]$ difference between the oxic region of the box and the OMZ, increasing as the gradient increases. Only oxic regeneration occurs in the open box and in the OMZ outside the SZ (with the exception that sedimentary denitrification also occurs in the open box). The SZ is divided further into two volumes, a volume housing

denitrification in which $[O_2]$ is <10 μmol/kg, and another volume housing oxic respiration in which $[O_2]$ is equivalent to that in the OMZ outside the SZ; the relative sizes of these volumes is determined by the mean $[O_2]$ of the SZ. Of the organic matter received by a box, the OMZ and SZ receive fractions for regeneration that are greater than their fractional areas by a calculated factor, in line with the tendency for suboxic zones to occur below regions of upwelling (Deutsch et al., 2004); this factor decreases toward 1 as the horizontal cross-sectional area of the OMZ grows. The changes in the volumes of SZ and OMZ occur through reassignments of quantities of water between the relevant volumes. Exchange of water among the volumes is parameterized to increase with the cross-sectional areas of the OMZ and SZ, as intercepted by a nearly horizontal advective flow.

A.2. Sedimentary denitrification parameterization

We assume a power law relation based on Martin et al. (1987) for the downward decrease in the organic matter flux to the seafloor, and seafloor hypsometry is taken from Menard and Smith (1966). This yields a benthic denitrification rate for each box. In order to match the modern depth distribution of sedimentary denitrification derived by Middelburg et al. (1996), we must roughly match their depth distribution of organic matter flux to the seabed, which yields higher fluxes than the Martin et al. relation at any given water depth (for instance, 10-fold higher at 1000 m). We thus alter the parameters in the Martin et al. relation, so that organic matter flux matches that used by Middelburg et al. at 3500 m. However, for the entire depth range of the ocean, this still results in much less organic matter flux to the seabed in our model than in the study of Middelburg et al. As a result, our model's rate of sedimentary denitrification is less than that of Middelburg et al. The likely reason for this discrepancy between Martin et al. and Middelburg et al. is that sedimentary margins, the environment considered by Middelburg et al., tend to have higher organic matter delivery at a given water depth than in the open ocean. Since water column denitrification is also focused along ocean margins, this discrepancy also speaks

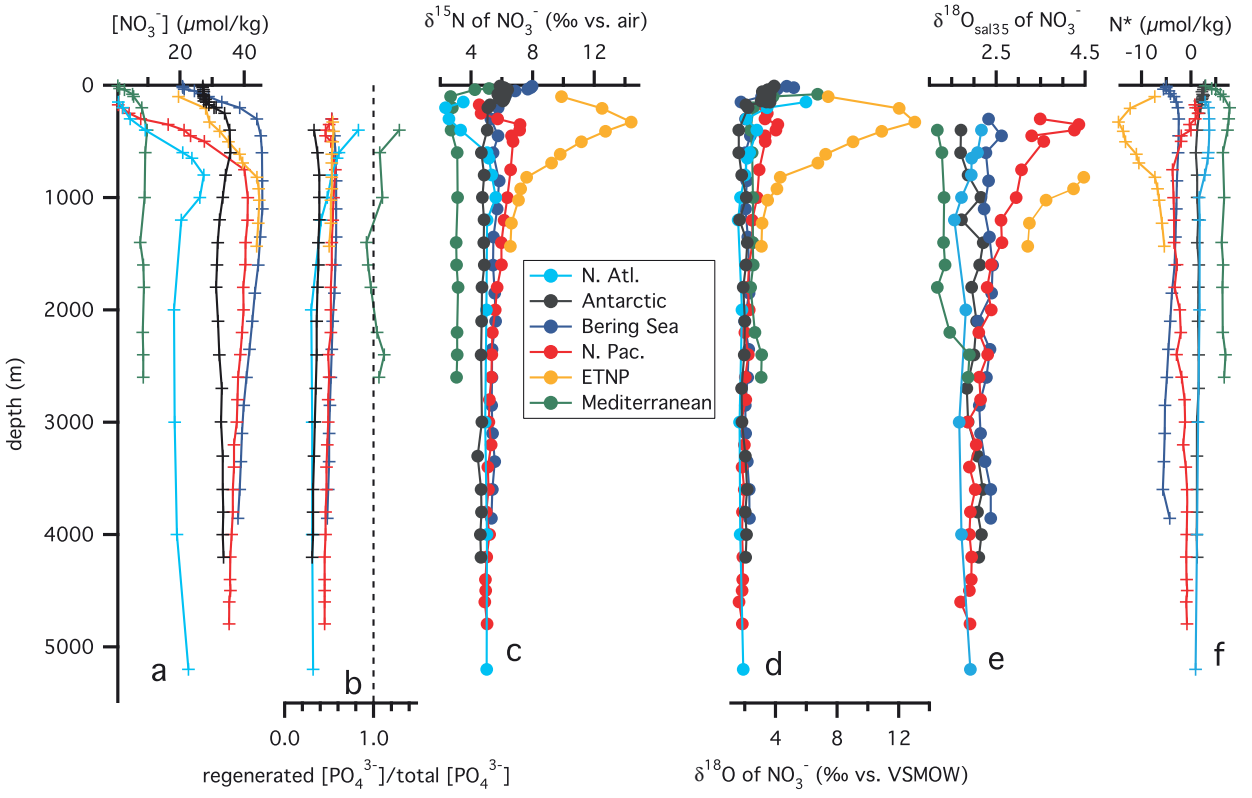

Fig. A1. Depth profiles from the following sites across the global ocean: (2) the Sargasso Sea at a station along the Bermuda Atlantic Time Series Validation Cruise 32 (labeled N. Atl.; 19.4°N, 65.0°W; (Knapp et al., 2008)), (3) the Pacific sector of the Antarctic Zone in the Southern Ocean, south of Australia (labeled Antarctic; 56.9°S, 139.9°E), collected during Clivar SR3, (4) the central Bering Sea basin (54.8°N, 179.7°E; (Lehmann et al., 2005)), (5) Hawaii Ocean Time-series Station Aloha (labeled N. Pac., (Sigman et al., 2009)), (6) the eastern tropical North Pacific west of the tip of Baja California (labeled ETNP) (Sigman et al., 2005); the western Mediterranean (36.6°N, 0.3°W), collected during Almofront Cruise 2 (Pantoja et al., 2002). Parameters plotted are (a) nitrate concentration, (b) the concentration ratio of regenerated to total phosphate, (c, d) the $\delta^{15}N$ and $\delta^{18}O$ of nitrate, (e) the salinity corrected $\delta^{18}O$, and (f) N*. For the "salinity corrected" nitrate $\delta^{18}O$ (Knapp et al., 2008), we assume a constant $\Delta\delta^{18}O/\Delta S$ of 0.5 and correct all samples to a salinity of 35‰. This relationship fails to capture the effects of sea ice formation and glacial runoff; however, this is the relationship assumed in the model, so we use it with the data for consistency. One exception here is the Mediterranean, which is not included in the box model, and which has a very high deep salinity, reaching above 38 psu. For it, we take the $\delta^{18}O$ relative to the deep North Atlantic from a global atlas of water $\delta^{18}O$ (LeGrande and Schmidt, 2006).

to the low rate of water column denitrification in the model (see Section 2.2).

Appendix B. Isotope methods and ancillary data

B.1. Isotope methods

The $^{15}N/^{14}N$ and $^{18}O/^{16}O$ of NO_3^- were determined using the denitrifier method (Casciotti et al., 2002; Sigman et al., 2001). NO_3^- is converted quantitatively to N_2O by a strain of bacterial denitrifier that lacks nitrous oxide reductase activity, and the product N_2O is extracted, purified, and analyzed by continuous flow isotope ratio mass spectrometry. Individual analyses are referenced to injections of N_2O from a pure gas cylinder and then standardized using international NO_3^- isotopic reference material IAEA-N3, which we take to have a $\delta^{15}N$ of 4.7‰ vs. air (Gonfiantini et al., 1995) and a $\delta^{18}O$ of 25.6‰ vs. VSMOW (Böhlke et al., 2003). The O isotope data are corrected for oxygen isotope exchange with water during reduction of NO_3^- to N_2O as well as for the analysis blank.

For the data reported here, the isotope scale contraction due to the exchange term was estimated using ^{18}O-enriched water (Casciotti et al., 2002), because many of the analyses were done before the $\delta^{18}O$ of a second nitrate O isotope reference material had been reported and reliably tested (Revesz and Böhlke, 2002; Revesz et al., 1997; Silva et al., 2000). More recently, on-line pyrolysis of nitrate isotope reference materials (Böhlke et al., 2003) has allowed for the use of multiple nitrate isotope reference materials (Casciotti et al., 2007; Mcilvin and Altabet, 2005). We have adopted the use of IAEA-N3 and USGS-34 reference materials (with assigned $\delta^{18}O$ of 25.61‰ and -27.93‰ (Böhlke et al., 2003)). We have compared the two referencing schemes (the older enriched water-based scheme and the newer bracketing reference-based scheme) in two ways. First, on individual days, samples were referenced to VSMOW by both schemes. Second, samples previously run and referenced with the old (enriched water-based) scheme were reanalyzed, referencing with the new (bracketing reference-based) scheme. Both comparison approaches indicate that deep ocean samples corrected with the new (bracket reference-based) scheme result in lower $\delta^{18}O$ values than when corrected with old (enriched water-based) scheme. The first comparison approach (using both correction schemes on individual days of analysis) yield a $\delta^{18}O$ difference of 0.65‰, whereas the second correction approach (recent reanalyses of samples using the new correction scheme) indicate a difference of 0.57‰. These estimates of the difference are consistent with one another and consistent with calculations of the "contraction factor" by the two methods, with the bracketing scheme indicating that a greater contraction factor is needed than indicated by the enriched water referencing scheme, which would suggest that the latter will place the $\delta^{18}O$ of deep water samples at values too close to IAEA-N3 and thus too high in $\delta^{18}O$. Throughout, we correct the data referenced with the old scheme in a way that shifts deep ocean samples down in $\delta^{18}O$ by very close to 0.60‰ (the correction being proportional to the measured difference from the $\delta^{18}O$ of IAEA-N3), consistent with results described above. One exception to this is the Bering Sea profile, which was corrected downward by an additional 0.5‰ to address a previous under-correction, as verified by subsequent tests.

Over the evolution of the different isotope correction schemes, replicate analyses have suggested an uncertainty in the measurements of ± 0.2‰ for $\delta^{15}N$ and ± 0.5‰ for $\delta^{18}O$ (1SD); using the current scheme, daily analyses of a deep North Pacific sample suggest a 1SD of ± 0.2‰ for $\delta^{15}N$ and ± 0.4‰ for $\delta^{18}O$. The isotope values for samples reported here derive from at least duplicate analysis, yielding standard errors of better than ± 0.1‰ for $\delta^{15}N$ and ± 0.3‰ for $\delta^{18}O$.

The precision of O isotope data is greater within individual analysis runs than between runs, such that systematic errors can exist between profiles due to analysis in separate runs. Thus, to specifically target isotopic differences among deep waters from different regions, subsequent to and independent from the generation of the profile data, we have conducted four individual analysis runs in which four samples are taken from the deep section of each of the profiles and analyzed together. The data from the comparison runs were all corrected with the current scheme of bracketing references. The results from these 'comparison' runs are reported in Table 2 and plotted along with profile averages in Fig. 9. The depths (in m) comprising the comparison samples are as follows: Atl.: 1200, 2000, 3000, 4000; AA: 1800, 2100, 2400, 3000; HOT: 3800, 4200, 4400, 4600; Ber.: 2100, 2350, 2600, 2850; Med: 1600, 1800, 2200, 2400.

The model includes salinity-associated water $\delta^{18}O$ variation, so the model/data comparison does not necessarily call for any normalization of the nitrate $\delta^{18}O$ data for variation in seawater $\delta^{18}O$. However, the box model fails to capture some important salinity variations in the ocean, such as the halocline in the Bering Sea. Thus, in several cases, we include a salinity-corrected version of the nitrate $\delta^{18}O$ data alongside the original data. The correction is applied only below 300 m, and it is applied only to the regenerated nitrate fraction in a sample, that is, the fraction of the nitrate that was clearly produced in water with the in situ $\delta^{18}O$. The correction is uniformly based on the deviation of in situ salinity from 35 psu (close to the salinity of the deep North Atlantic), and the assumed $\Delta\delta^{18}O/\Delta S$ relationship is the same as in the model. The one exception is for the Mediterranean, which is not explicitly included in the model and has a very high salinity, ~38 psu. The global water $\delta^{18}O$ database of (LeGrande and Schmidt, 2006) indicates that the deep Mediterranean has a $\delta^{18}O$ that is 1.45‰ vs. VSMOW, and this is used to estimate a $\delta^{18}O$ of 1.15‰ for nitrification relative to ambient water.

B.2. Ancillary data and averages

Hydrographic and nutrient data were retrieved from the same stations as the isotopic data, with the exception of the North Atlantic profile, for which $[O_2]$ and $[PO_4^{3-}]$

were taken from a nearby station from the WOCE A22 line. Potential temperature was calculated from the UNESCO 1983 equation of in situ temperature, salinity, and pressure. Preformed [O_2] was calculated from salinity and potential temperature, using the solubility equation of Weiss (1970). Regenerated phosphate was estimated by differencing the preformed and *in situ* [O_2] and then multiplying by a factor of 1:170. Average isotopic values for profiles are calculated by averaging over the depth ranges of 300–1500 m (intermediate) or 1500 m – bottom (deep), weighting for nitrate concentration and depth spacing between samples. The Antarctic profile is from poleward of the latitude of intermediate water formation; thus, the entire profile from 300 m to the bottom was averaged and considered as a deep value.

Appendix C. Additional model experiment

N cycle-only case with O_2 incorporation into nitrate (experiment I.D. from Table 3): We assume here that, in nitrification, O_2 supplies 1 out of the 6 oxygen atoms to nitrate. All else held constant, [O_2] decreases as regenerated nitrate accumulates, and isotopic fractionation during O_2 respiration causes the $\delta^{18}O$ of O_2 to increase (Fig. 4c, g). This works against the tendency for subsurface nitrate $\delta^{18}O$ to decrease with increasing regenerated nitrate and phosphate. In the model, this weakens the correlation of nitrate $\delta^{18}O$ with phosphate concentration and with the fraction of regenerated-to-total phosphate (Fig. 4d, h). In the deep ocean, the trend is maintained at near the "water-only" case (Section 3.1.) from the deep North Atlantic to the Southern Ocean and Indian Ocean, but it is reversed from the Indian basin to the North Pacific (Fig. 4d, h, filled blue squares). At the intermediate box level, the Atlantic-to-North Pacific trend from the "water-only" case is essentially removed (Fig. 4d, h, filled red circles). The mean $\delta^{18}O$ of nitrate in the ocean is 6.9‰ vs. SMOW, elevated by ~6‰ relative to the "water-only" case, due to the high $\delta^{18}O$ of dissolved O_2 relative to that of ocean water (~24‰ higher at the surface). This absolute value clearly disagrees with deep ocean nitrate $\delta^{18}O$ measurements. However, we have assumed no fractionation during the incorporation of oxygen atoms from O_2 into nitrate, whereas there could well be a significant fractionation, so this disagreement is as yet not a meaningful constraint.

References

Altabet, M.A., Pilskaln, C., Thunell, R., Pride, C., Sigman, D., Chavez, F., Francois, R., 1999. The nitrogen isotope biogeochemistry of sinking particles from the margin of the eastern North Pacific. Deep-Sea Research I—Oceanographic Research Papers 46, 655–679.

Bender, M.L., 1990. The $\delta^{18}O$ of dissolved O_2 in seawater—a unique tracer of circulation and respiration in the deep-sea. Journal of Geophysical Research—Oceans 95 (C12), 22243–22252.

Böhlke, J.K., Ericksen, G.E., Revesz, K., 1997. Stable isotope evidence for an atmospheric origin of desert nitrate deposits in northern Chile and southern California. Chemical Geology 136, 135–152.

Böhlke, J.K., Mroczkowski, S.J., Coplen, T.B., 2003. Oxygen isotopes in nitrate: new reference materials for O-18 : O-17 : O-16 measurements and observations on nitrate-water equilibration. Rapid Communications in Mass Spectrometry 17 (16), 1835–1846.

Brandes, J.A., Devol, A.H., 1997. Isotopic fractionation of oxygen and nitrogen in coastal marine sediments. Geochimica et Cosmochimica Acta 61 (9), 1793–1801.

Brandes, J.A., Devol, A.H., 2002. A global marine fixed nitrogen isotopic budget: implications for Holocene nitrogen cycling. Global Biogeochemical Cycles 16 (4), 1120, doi:10.1029/2001GB001856.

Brandes, J.A., Devol, A.H., Yoshinari, T., Jayakumar, D.A., Naqvi, S.W.A., 1998. Isotopic composition of nitrate in the central Arabian Sea and eastern tropical North Pacific: a tracer for mixing and nitrogen cycles. Limnology and Oceanography 43 (7), 1680–1689.

Carpenter, E., Harvey, H., Fry, B., Capone, D., 1997. Biogeochemical tracers of the marine cyanobacterium Trichodesmium. Deep-Sea Research I 44 (1), 27–38.

Casciotti, K.L., Böhlke, J.K., McIlvin, M.R., Mroczkowski, S.J., Hannon, J.E., 2007. Oxygen isotopes in nitrite: analysis, calibration, and equilibration. Analytical Chemistry 79 (6), 2427–2436.

Casciotti, K.L., Sigman, D.M., Hastings, M.G., Böhlke, J.K., Hilkert, A., 2002. Measurement of the oxygen isotopic composition of nitrate in seawater and freshwater using the denitrifier method. Analytical Chemistry 74 (19), 4905–4912.

Casciotti, K.L., Trull, T.W., Glover, D.M., Davies, D., 2008. Constraints on nitrogen cycling at the subtropical North Pacific Station ALOHA from isotopic measurements of nitrate and particulate nitrogen. Deep-Sea Research II—Topical Studies in Oceanography 55 (14-15), 1661–1672.

Cline, J.D., Kaplan, I.R., 1975. Isotopic fractionation of dissolved nitrate during denitrification in the Eastern Tropical North Pacific Ocean. Marine Chemistry 3, 271–299.

Conkright, M.E., Locarnini, R.A., Garcia, H.E., O'Brien, T.D., Boyer, T.P., Stephens, C., Antonov, J.I., 2002. World Ocean Atlas 2001: Objective Analyses, Data Statistics, and Figures, CD-ROM Documentation. National Oceanographic Data Center, Silver Spring.

Delwiche, C.C., Zinke, P.J., Johnson, C.M., Virginia, R.A., 1979. Nitrogen isotope distribution as a presumptive indicator of nitrogen-fixation. Botanical Gazette 140, 65–69.

Deutsch, C., Gruber, N., Key, R.M., Sarmiento, J.L., Ganaschaud, A., 2001. Denitrification and N_2 fixation in the Pacific Ocean. Global Biogeochemical Cycles 15 (2), 483–506.

Deutsch, C., Sarmiento, J.L., Sigman, D.M., Gruber, N., Dunne, J.P., 2007. Spatial coupling of nitrogen inputs and losses in the ocean. Nature 445 (7124), 163–167.

Deutsch, C., Sigman, D.M., Thunell, R.C., Meckler, N., Haug, G.H., 2004. Stable isotope constraints on the glacial/interglacial oceanic nitrogen budget. Global Biogeochemical Cycles 18 (GB4012).

DiFiore, P.J., Sigman, D.M., Trull, T.W., Lourey, M.J., Karsh, K.L., Cane, G., Ho, R., 2006. Nitrogen isotope constraints on Subantarctic biogeochemistry. Journal of Geophysical Research—Oceans 111 (C08016), doi:10.1029/2005JC003216.

Gonfiantini, R., Stichler, W., Rosanski, K., 1995. Standards and Intercomparison Materials Distributed by the IAEA for Stable Isotope Measurements. International Atomic Energy Agency, Vienna.

Granger, J., Sigman, D.M., Lehmann, M.F., Tortell, P.D., 2008. Nitrogen and oxygen isotope fractionation during dissimilatory nitrate reduction by denitrifying bacteria. Limnology and Oceanography 53 (6), 2533–2545.

Granger, J., Sigman, D.M., Needoba, J.A., Harrison, P.J., 2004. Coupled nitrogen and oxygen isotope fractionation of nitrate during assimilation by cultures of marine phytoplankton. Limnology and Oceanography 49 (5), 1763–1773.

Gruber, N., 2004. The dynamics of the marine nitrogen cycle and its influence on atmospheric CO_2 variations. In: Oguz, M.F.a.T. (Ed.), Carbon-Climate Interactions. Wiley, New York, pp. 1–39.

Gruber, N., Sarmiento, J.L., 1997. Global patterns of marine nitrogen fixation and denitrification. Global Biogeochemical Cycles 11, 235–266.

Hoering, T., Ford, H.T., 1960. The isotope effect in the fixation of nitrogen by Azotobacter. Journal of the American Chemical Society 82, 376–378.

Ito, T., Follows, M.J., 2005. Preformed phosphate, soft tissue pump and atmospheric CO_2. Journal of Marine Research 63 (4), 813–839.

Jenkins, W.J., Doney, S.C., 2003. The subtropical nutrient spiral. Global Biogeochemical Cycles 17 (4) article no. 1110.

Keir, R.S., 1988. On the late Pleistocene ocean geochemistry and circulation. Paleoceanography 3, 413–445.

Kendall, C., 1998. Tracing nitrogen sources and cycling in catchments. In: Kendall, C., McDonnell, J.J. (Eds.), Isotope Tracers in Catchment Hydrology. Elsevier, New York, pp. 519–576.

Knapp, A.N., DiFiore, P.J., Deutsch, C., Sigman, D.M., Lipschultz, F., 2008. Nitrate isotopic composition between Bermuda and Puerto Rico:

implications for N_2 fixation in the Atlantic Ocean. Global Biogeochemical Cycles 22 (3), GB3014.
Kuypers, M.M.M., Lavik, G., Woebken, D., Schmid, M., Fuchs, B.M., Amann, R., Jørgensen, B.B., Jetten, M.S.M., 2005. Massive nitrogen loss from the Benguela upwelling system through anaerobic ammonium oxidation. Proceedings of the National Academy of Sciences of the United States of America 102, 6478–6483.
Laws, E.A., Falkowski, P.G., Smith, W.O., Ducklow, H., McCarthy, J.J., 2000. Temperature effects on export production in the open ocean. Global Biogeochemical Cycles 14 (4), 1231–1246.
LeGrande, A.N., Schmidt, G.A., 2006. Global gridded data set of the oxygen isotopic composition in seawater. Geophysical Research Letters 22 (L12604).
Lehmann, M.F., Sigman, D.M., Berelson, W.M., 2004. Coupling the N-15/N-14 and O-18/O-16 of nitrate as a constraint on benthic nitrogen cycling. Marine Chemistry 88 (1–2), 1–20.
Lehmann, M.F., Sigman, D.M., McCorkle, D.C., Brunelle, B.G., Hoffmann, S., Kienast, M., Cane, G., Clement, J., 2005. Origin of the deep Bering Sea nitrate deficit: constraints from the nitrogen and oxygen isotopic composition of water column nitrate and benthic nitrate fluxes. Global Biogeochemical Cycles 19 (4), GB4005.
Lehmann, M.F., Sigman, D.M., McCorkle, D.C., Granger, J., Hoffmann, S., Cane, G., Brunelle, B.G., 2007. The distribution of nitrate $^{15}N/^{14}N$ in marine sediments and the impact of benthic nitrogen loss on the isotopic composition of oceanic nitrate. Geochimica et Cosmochimica Acta 71, 5384–5404.
Levine, N.M., Bender, M.L., Doney, S.C., 2009. The delta O-18 of dissolved O_2 as a tracer of mixing and respiration in the mesopelagic ocean. Global Biogeochemical Cycles 23, GB1006.
Liu, K.-K., Kaplan, I.R., 1989. The eastern tropical Pacific as a source of 15N-enriched nitrate in seawater off southern California. Limnology and Oceanography 34, 820–830.
Martin, J.H., Knauer, G.A., Karl, D.M., Broenkow, W.W., 1987. VERTEX: carbon cycling in the northeast Pacific. Deep-Sea Research 34 (2), 267–285.
Matsumoto, K., Sarmiento, J.L., Brzezinski, M.A., 2002. Silicic acid 'leakage' from the Southern Ocean as a possible mechanism for explaining glacial atmospheric pCO_2. Global Biogeochemical Cycles 16 (3), 1031, doi:10.1029/2001GB001442.
Mcilvin, M.R., Altabet, M.A., 2005. Chemical conversion of nitrate and nitrite to nitrous oxide for nitrogen and oxygen isotopic analysis in freshwater and seawater. Analytical Chemistry 77 (17), 5589–5595.
Menard, H.W., Smith, S.M., 1966. Hypsometry of ocean basin provinces. Journal of Geophysical Research 71, 4305–4325.
Middelburg, J.J., Soetaert, K., Herman, P.M.J., Heip, C.H.R., 1996. Denitrification in marine sediments: a model study. Global Biogeochemical Cycles 10 (4), 661–673.
Orsi, A.H., Whitworth, T.W., Nowlin, W.D., 1995. On the meridional extent and fronts of the Antarctic Circumpolar Current. Deep-Sea Research I—Oceanographic Research Papers 42 (5), 641–673.
Pantoja, S., Repeta, D.J., Sachs, J.P., Sigman, D.M., 2002. Stable isotope constraints on the nitrogen cycle of the Mediterranean Sea water column. Deep-Sea Research I 4, 1609–1621.
Revesz, K., Böhlke, J.K., 2002. Comparison of deltaO18 measurements in nitrate by different combustion techniques. Analytical Chemistry 74 (20), 5410–5413.
Revesz, K., Böhlke, J.K., Yoshinari, Y., 1997. Determination of $\delta^{18}O$ and $\delta^{15}N$ in nitrate. Analytical Chemistry 69, 4375–4380.
Robinson, R.S., Sigman, D.M., DiFiore, P.J., Rohde, M.M., Mashiotta, T.A., Lea, D.W., 2005. Diatom-bound N-15/N-14: new support for enhanced nutrient consumption in the ice age subantarctic. Paleoceanography 20 (3), PA3003.
Sebilo, M., Billen, G., Grably, M., Mariotti, A., 2003. Isotopic composition of nitrate-nitrogen as a marker of riparian and benthic denitrification at the scale of the whole Seine River system. Biogeochemistry 63 (1), 35–51.
Sigman, D.M., Altabet, M.A., Francois, R., McCorkle, D.C., Fischer, G., 1999. The $\delta^{15}N$ of nitrate in the Southern Ocean: consumption of nitrate in surface waters. Global Biogeochemical Cycles 13 (4), 1149–1166.
Sigman, D.M., Altabet, M.A., McCorkle, D.C., Francois, R., Fischer, G., 2000. The $\delta^{15}N$ of nitrate in the Southern Ocean: nitrogen cycling and circulation in the ocean interior. Journal of Geophysical Research 105 (C8), 19,599–19,614.
Sigman, D.M., Casciotti, K.L., Andreani, M., Barford, C., Galanter, M., Bohlke, J.K., 2001. A bacterial method for the nitrogen isotopic analysis of nitrate in seawater and freshwater. Analytical Chemistry 73 (17), 4145–4153.
Sigman, D.M., DiFiore, P. J., Hain, M.P., Deutsch, C., Karl, D.M., 2009. Sinking organic matter spreads the nitrogen isotope signal of pelagic denitrification in the North Pacific. Geophysical Research Letters, 36, L08605, doi:10.1029/2008GL035784.
Sigman, D.M., Granger, J., DiFiore, P.J., Lehmann, M.F., Geen, A.v., Ho, R., Cane, G., 2005. Coupled nitrogen and oxygen isotope measurements of nitrate along the eastern North Pacific margin. Global Biogeochemical Cycles 19 (GB4022).
Sigman, D.M., Haug, G.H., 2003. Biological pump in the past. In: Elderfield, H. (Ed.), Treatise On Geochemistry, vol. 6: The Oceans and Marine Geochemistry. Elsevier Pergamon, Oxford, pp. 491–528.
Sigman, D.M., Lehman, S.J., Oppo, D.W., 2003a. Evaluating mechanisms of nutrient depletion and C-13 enrichment in the intermediate-depth Atlantic during the last ice age. Paleoceanography 18 (3), 1072, doi:10.1029/2002PA000818.
Sigman, D.M., McCorkle, D.C., Martin, W.R., 1998. The calcite lysocline as a constraint on glacial/interglacial low-latitude production changes. Global Biogeochemical Cycles 12 (3), 409–427.
Sigman, D.M., Robinson, R., Knapp, A.N., van Geen, A., McCorkle, D.C., Brandes, J.A., Thunell, R.C., 2003b. Distinguishing between water column and sedimentary denitrification in the Santa Barbara Basin using the stable isotopes of nitrate. Geochemistry, Geophysics, Geosystems 4 (5), 1040.
Silva, S.R., Kendall, C., Wilkison, D.H., Ziegler, A.C., Chang, C.C.Y., Avanzino, R.J., 2000. A new method for collection of nitrate from fresh water and the analysis of nitrogen and oxygen isotope ratios. Journal of Hydrology 228, 22–36.
Toggweiler, J.R., Murnane, R., Carson, S., Gnanadesikan, A., Sarmiento, J.L., 2003. Representation of the carbon cycle in box models and GCMs: 2, organic pump. Global Biogeochemical Cycles 17 (1), 1027.
Tyrrell, T., 1999. The relative influences of nitrogen and phosphorus on oceanic primary production. Nature 400, 525–531.
Voss, M., Dippner, J.W., Montoya, J.P., 2001. Nitrogen isotope patterns in the oxygen-deficient waters of the Eastern Tropical North Pacific Ocean. Deep-Sea Research I—Oceanographic Research Papers 48 (8), 1905–1921.
Weiss, R.F., 1970. The solubility of nitrogen, oxygen and argon in water and seawater. Deep-Sea Research 17, 721–735.